



**PROCESS IMPROVEMENTS FOR THE AH-64 TAIL ROTOR  
VIBRATION ANALYSIS**

THESIS

Mark C Newkirk, Lieutenant Commander, USN

AFIT/GAE/ENY/07-J15

**DEPARTMENT OF THE AIR FORCE  
AIR UNIVERSITY**

**AIR FORCE INSTITUTE OF TECHNOLOGY**

**Wright-Patterson Air Force Base, Ohio**

APPROVED FOR PUBLIC RELEASE; DISTRIBUTION UNLIMITED

The views expressed in this thesis are those of the author and do not reflect the official policy or position of the United States Air Force, Department of Defense, or the United States Government.

**PROCESS IMPROVEMENTS FOR THE AH-64 TAIL ROTOR  
VIBRATION ANALYSIS**

THESIS

Presented to the Faculty

Department of Aeronautics and Astronautics

Graduate School of Engineering and Management

Air Force Institute of Technology

Air University

Air Education and Training Command

In Partial Fulfillment of the Requirements for the  
Degree of Master of Science in Aeronautical Engineering

Mark C. Newkirk, BAS

Lieutenant Commander, USN

June 2007

APPROVED FOR PUBLIC RELEASE; DISTRIBUTION UNLIMITED

AFIT/GAE/ENY/07-J15

**PROCESS IMPROVEMENTS FOR THE AH-64 TAIL ROTOR**  
**VIBRATION ANALYSIS**

Mark C. Newkirk, BAS  
Lieutenant Commander, USN

Approved:

<u>                    /Signed/                    </u>	<u>                    </u>
Prof. Donald L. Kunz (Chairman)	date

<u>                    /Signed/                    </u>	<u>                    </u>
Eric D. Swenson, Major, USAF (Member)	date

<u>                    /Signed/                    </u>	<u>                    </u>
Dr. Mark F. Reeder (Member)	date

### **Abstract**

The Apache was the first helicopter of its kind to fly with the tail rotor blade offset by 55 degrees as opposed to the traditional 90 degrees. Current balancing methods approximate the rotor system as a traditional 4 bladed, same plane system with different weight sensitivity coefficients for each set of blades. The Apache tail rotor computer model was built using the Rotorcraft Comprehensive Analysis System (RCAS) program. The objective was not to develop solutions for the sensitivity coefficients, but to identify predictive trends that result from the tail rotor blade location.

Currently, sensitivity coefficients applied to the adjustment algorithms of the Aviation Vibration Analyzer (AVA) processor are broken down into an outer blade coefficient and an inner blade coefficient. Evidence from the computer simulation results computed in this research showed that the sensitivities depended on the quadrant the phase fell into, not the relationship between the inner and outer blades. That would mean every blade would have two sensitivity coefficients, one for the adjacent 55 degree quadrant and one for the adjacent 125 degree quadrant. Information collected from RCAS provides enough validation that changes should be made in the process and the next steps should be taken to determining more accurate sensitivity coefficients for the Apache tail rotor balancing procedures.

## **Acknowledgements**

I could not have completed the journey of writing a thesis on my own. There were many times on the adventure when I needed to look to those who are closest to me for guidance and support. Their ability to believe in me and help me through the difficult times is why I was able to achieve this goal.

I would like to first acknowledge Dr. Kunz. Your dedication and commitment to this thesis kept me inspired and helped me believe that we were on the right path and we will find answers to the objectives. Thank you for your willingness to drop whatever you were doing and help steer me on the right course.

I would also like to thank Jon Keller for his time spent sharing his first hand knowledge on the Apache. Your knowledge of the subject matter allowed me ensure the hard work that went into building the model would produce a product that would be useful in the end.

I owe my greatest gratitude to my wife and family. You have helped me through the difficult times on this journey and your unwavering support and believing in me has allowed me to complete this endeavor. Thank you.

Mark C. Newkirk

## Table of Contents

	Page
Abstract.....	iv
Acknowledgements.....	v
List of Tables .....	x
List of Tables .....	x
I. Introduction .....	1
General.....	1
Problem Statement.....	2
Research Methodology .....	3
II. Background.....	4
History.....	4
Maintenance Test Flight .....	7
Tail Rotor Balancing.....	8
Apache Tail Rotor Vibration Analysis Procedure .....	10
III. Methodology.....	15
Rotorcraft Comprehensive Analysis System (RCAS) .....	15
RCAS Coordinate Systems.....	15
Structural Model .....	17
Aerodynamic Model .....	20
AH-64 Apache Tail Rotor Model .....	22

	Page
AH-64D Structural Model .....	23
Thrust .....	29
AH-64D Aerodynamic Model .....	34
Comparative Model and Data Output .....	37
IV: Results and Discussion .....	40
Introduction .....	40
Multiple Weights, Single Blade .....	41
Single Weight, Multiple Blades .....	44
Equal Weights Added to Adjacent Blades .....	47
Unequal Weights, Adjacent Blades .....	50
Accelerometer in the Y (Lateral) Direction .....	60
Accelerometer in the X (Longitudinal) Direction .....	61
Results and Analysis Conclusions .....	62
V: Conclusions .....	65
Conclusions of Research .....	65
Suggestions for Future Research .....	67
Bibliography .....	68
Appendix A: AH-64 Apache Tail Rotor RCAS Input File .....	70
Vita .....	85



## List of Figures

Figure	Page
Figure 1. AH-64 Apache Tail Rotor Hub and Rotor Blades	2
Figure 2. AH-64 Apache General Dimensions (7)	5
Figure 3. MIL MI-28 Scissor Tail Rotor Variant	7
Figure 4. RPM Sensor Installation (17)	12
Figure 5. Accelerometer and Tachometer Installation locations. (17)	13
Figure 6. RCAS Coordinate System's Schematic (6)	16
Figure 7. Block Diagram of the Physical Model (6)	17
Figure 8. Block Diagram of the Structural Model (6)	18
Figure 9. Aerodynamic Model Hierarchy (6)	22
Figure 10. Apache Structural Model	23
Figure 11. Rotational Sequence of the Tail Rotor Subsystem	25
Figure 12. Apache Tail Rotor Blade Mass Distribution (8)	27
Figure 13. Apache Tail Rotor Blade Chordwise Mass Moment Distribution (8)	28
Figure 14. Apache Tail Rotor Blade Beamwise Mass Moment Distribution (8)	29
Figure 15. Engine Nose Gearbox Efficiency Estimate (8)	31
Figure 16. Main Gearbox Efficiency Estimate (8)	32
Figure 17. Chart to Determine the Torque Required to Hover (7)	33
Figure 18. AH-64 Apache Tail Rotor Aerodynamic Model	34
Figure 19. Longbow Apache Tail Rotor Blade Planform and Twist Distribution (8)	37
Figure 20. Traditional – Multiple Weights, Single Blade – Z forces	42
Figure 21. Apache – Multiple Weights, Single Blade	43

	Page
Figure 22. Weight to Amplitude Relationship, Both Models	44
Figure 23. Traditional – Z force w/ 10g added 1 Blade at a Time	45
Figure 24. Apache – Z force w/ 10g added 1 Blade at a Time	46
Figure 25. Z forces on 82 lbf and 300 lbf of Thrust	47
Figure 26. Traditional Equal wt (10g) to Adjacent Blades	49
Figure 27. Apache Equal wt (10g) to Adjacent Blades	50
Figure 28. Traditional Rotor System 10g-4g Adjacent Blades	51
Figure 29. Apache Rotor System 10g-4g Adjacent Blades	52
Figure 30. Multiple Weights Added to No. 1 Inner Blade and the Bounding Blades of 3 Different Quadrant Sizes	53
Figure 31. 90 Degree Quadrant Weight to Amplitude Distribution	54
Figure 32. 55 Degree Quadrant Weight to Amplitude Distribution	55
Figure 33. 125 Degree Quadrant Weight to Amplitude Distribution	55
Figure 34. Slope Variation within a 90 Degree Quadrant	57
Figure 35. Slope Variation within a 55 Degree Quadrant	57
Figure 36. Slope Variation within a 125 Degree Quadrant	58
Figure 37. 0-180 Degree Phase Representation of Apache and Traditional Model	59
Figure 38. 55, 90, and 125 Degree Quadrants Based at Zero Phase	60
Figure 39. Apache Model Y Force Distribution	61
Figure 40. X Force, Apache Model Equal wt (10g) to Adjacent Blades	62

## List of Tables

Table	Page
Table 1 .....	40

## **I. Introduction**

### **General**

The AH-64A Apache was first delivered to the United States Army on the 26<sup>th</sup> of January 1984. In the past 23 years the Apache has played an integral role in numerous world events, including in the Operation Restore Hope in Somalia, Operation Desert Storm, peace keeping in Bosnia, and most recently in the Global War on Terrorism. In March 1997 McDonnell Douglas delivered the first 198 AH-64D Longbow Apaches to the Army. The tests demonstrated that the Longbow Apache is 400 percent more lethal (hitting more targets), 720 percent more survivable, and require one third less maintenance hours per flight hour compared to the AH-64A Apache. (16) Throughout the list of improvements and technological advances since inception, the tail rotor has remained unchanged.

The Apache was the first helicopter of its kind to fly with the tail rotor blades offset by 55 and 125 degrees as opposed to the traditional 90 degrees. Figure 1 shows the rotor hub configuration and the different quadrant sizes. The original reason for offsetting the blades was to properly mount the delta-3 hinge which allows the blades to simultaneously flap and feather. During the test and evaluation, it was also discovered that this configuration reduced the noise produced by the tail rotor. Like most advances in technology, there come new areas of uncertainty. The tail rotor system is no exception.



**Figure 1. AH-64 Apache Tail Rotor Hub and Rotor Blades**

### **Problem Statement**

The purpose of this study is to investigate the tail rotor balance vibration analysis methods for the AH-64A/D. The original request came from Aviation and Missile Research Development and Engineering Center (AMRDEC). The current balancing methods approximate the rotor system as a traditional 4-bladed, same plane system with different weight sensitivity coefficients for the inner and outer blades. The procedure utilizes one vertical accelerometer (single axis) to measure the amplitude and phase of the rotor system. The capability exists to measure the accelerations in the lateral direction and modifications can be made to orient an accelerometer in the longitudinal direction as well. In the past, the Army has run into situations where some Apaches do not respond well to the calculated adjustments using the current single plane solution. The objective is not to develop solutions for the sensitivity coefficients, but to identify predictive trends that result from the tail rotor blade location.

## **Research Methodology**

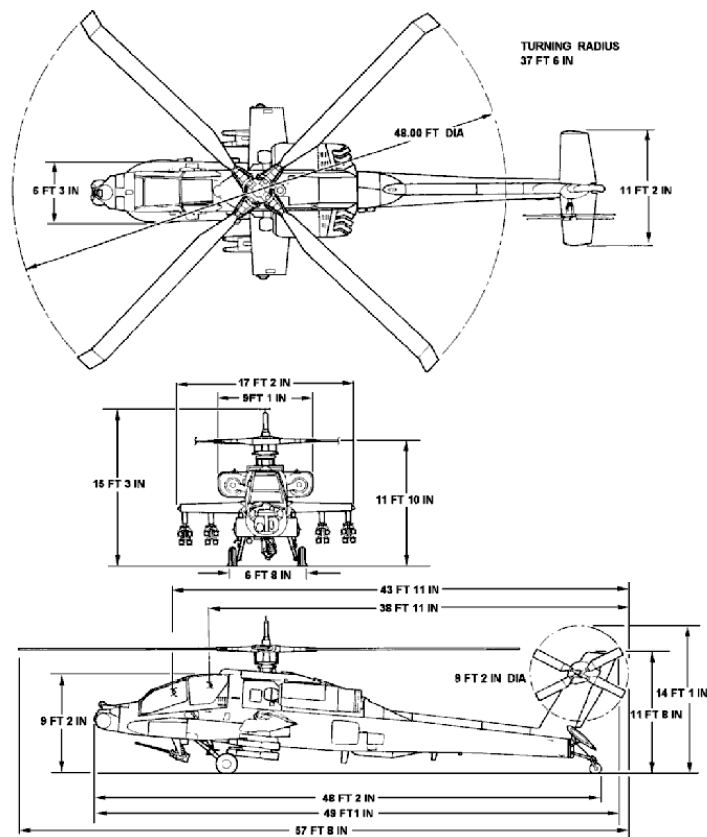
The objective of this research was to build and analyze a computer model of the Apache tail rotor system. According to AMRDEC, it was determined that a detailed computer model of the Apache tail rotor had never been created in the Rotorcraft Comprehensive Analysis System (RCAS) program. (6) The RCAS program is intended to serve as the standard for rotorcraft analysis; therefore it was the obvious choice of programs to use to analyze the tail rotor. The first objective was to determine if the tail rotor model responded differently than a traditional tail rotor. The second objective was to determine if there was a correlation between a traditional rotor system and the Apache rotor system.

## **II. Background**

### **History**

The Army's AH-64A Apache was first designed by the former Hughes Aircraft's Toolco Aircraft Division after responding to the Department of Defense's Request For Proposals for an Advanced Attack Helicopter in 1972. In September 1975 the prototype, YAH-64 had its first flight. Since 1975, the Apache contract has been represented under 4 different company names, currently the program is owned by Boeing. The US Government purchased 827 AH-64A of which 530 were to be remanufactured into AH-64D's. Since 1990 the AH-64 Apache has been sold to a total of eight other countries.

Figure 2 identifies the dimensions of the AH-64 Apache. The main rotor diameter is 48 ft and the tail rotor diameter is 9.17 ft. According to Raymer, a helicopter's tail rotor is typically 15-20% of the main rotor's diameter. (13:643) In the case of the Apache, the tail rotor is 19.1% the size of the main rotor. The Apache tail rotor consists of two teetering hubs and two blades on each hub. The inner hub is located 2.47 feet from the center of the fuselage and the outer hub is located 2.96 feet. Each pair of blades are teetering, semi-rigid and have delta-three hinges. (14) An H-60 Blackhawk's blades are mounted exactly 90 degrees apart in azimuth. The Apache's tail rotor hubs are offset 55 degrees allowing for two 55 degree gaps and two 125 degree gaps shown in the profile view in Figure 2.



General dimensions, AH-64A

**Figure 2. AH-64 Apache General Dimensions (7)**

The tail rotor flapping is not controlled laterally or longitudinally only the pitch is controlled. When the pilot adds an input to the pedals a cable mechanism transfers the input collectively to the tail pitch control mechanism. This mechanism is connected to the blades with pitch bearings and pitch links which transfer the inputs to the blades via the swashplate. When both pedals are centered (50% pedal input), the blades have a built in collective pitch of 7.4 degrees.



A teetering rotor system consists of two interconnected blades that form one structure with a flapping hinge at the shaft axis. The teetering hinge does not have independent flap or lead lag hinges. According to Leishman, “The teetering design has the advantage of being mechanically simple with a low parts count and it is easy to maintain. One disadvantage of the design is that it can have a relatively high parasitic drag in forward flight, in part because of the stabilizer bar.” (5) The Bell UH-1 Huey helicopter has a teetering main rotor system that utilizes a stabilizer bar. The stabilizer bar acts like a gyroscope providing increased flight stability. The tail rotor on the Apache has a total of four blades. Stabilizer bars are generally not found on four bladed teetering rotor systems since the addition of two more blades minimizes the vibratory loads and reduces the propagated noise from the rotor system. (5)

One of the distinct features of the Apache tail rotor is the fact that the blades do not have the standard 90 degree (perpendicular) phase separation. The separation between the span lines of the rotor blades is alternatively 55 degrees and 125 degrees. The arrangement of the blade location is due to the use of a “delta-three-hinge” which allows for the blades to simultaneously flap and feather. (15)

The Apache is the only American made helicopter that possesses a scissor like tail rotor. The Russians first included a scissor tail rotor configuration on the MIL MI-28 Havoc. The first prototype of the Havoc, developed at the Mil Moskow Helicopter Plant, flew in 1982, five years after the first flight of the Apache. The MI-28 was originally designed as a light combat helicopter. The Havoc’s production was limited after the Soviet Air Force chose the KA-50 Hokum A as their future combat helicopter. The tail

rotor of the MI-28 are 2 independent rotors with two blades each set at 35/145 degrees apart. (16)



**Figure 3. MIL MI-28 Scissor Tail Rotor Variant**

### **Maintenance Test Flight**

Specific maintenance actions on an aircraft will require it to complete a maintenance test flight (MTF). A test flight determines the proper functions of all the helicopter's systems. The systems checked include engine performance, stability and control, avionics, and vibration analysis. A typical helicopter can spend approximately 4-5% of its lifetime hours on maintenance test flights, and that does not account for the time spent on the ground, only airborne. Only the actual "flight" hours of an aircraft are recorded, so it is impossible to accurately determine the amount of time spent performing the ground procedures of an MTF. Based on experience, approximately half of the time spent on a maintenance test flight is spent on the ground performing such functions as verifying the functionality of the avionics systems and track and balancing of both the main and tail rotor.

Unlike the main rotor system, where both the tracking and balance vibration analysis are performed, the tail rotor only focuses on balancing. Earlier methods of balancing consisted of only static mass balancing of the rotor trying to make the weight as symmetrical as possible, however the aerodynamic effects also played a role in an imbalanced rotor. The current method of balancing an Apache's tail rotor involves adding and removing weights from the tip section of each individual blade. There are two pockets on the tip that hold adjustment weights, a forward and aft pocket. Weights are equally split between the pockets with half the weight adjusted made to the forward pocket and half the weight adjusted made to the aft pocket. (17) An accelerometer is used to measure the accelerations in vertical direction. An optical tachometer is also used to provide an accurate RPM reading. Approximately 40-50 revolutions of data are collected from the tail accelerometer and tail tachometer. Upon completion of a test run, the Aviation Vibration Analysis (AVA) computer provides data in the form of vibration amplitude in ips or inches per second. (12)

### **Tail Rotor Balancing**

After determining that statically balancing the blade in order to make the rotor as symmetrical as possible was not a feasible solution, blades had to not only been balanced by mass, but also aerodynamically. Rotor systems are now capable of having a plethora of adjustment options. Some of the more common techniques include adjustable pitch links, physically bendable trim tabs, and weight adjustments.

Vibration balancing equipment provides the technician with amplitude displayed in ips (inches per second) which has been established as the industry standard. The

accelerometer measures in units of gravity (g's). The data is then broken down into each revolution based on the tachometer. All of the revolutions are averaged together and a fast Fourier transform is applied to transform the data from the time domain into a frequency domain, it is then integrated to get a 1 per revolution ips and phase angle. (12)

The vibration equipment used by the Apache is the Aviation Vibration Analyzer (AVA). The AVA uses a non-learning linear algorithm to calculate corrections, meaning that the adjustments rely on an empirical database of responses to adjustments made specifically by an aircraft type. The algorithm calls on the database information when developing an adjustment solution for the particular vibration and phase angle on the aircraft. (2) This type of algorithm assumes that there is a linear relationship between the adjustment and the resultant change, which allows for a simplification of the calculations. However, the average coefficient matrix is only about 20% accurate. Many factors like electronic noise, weather, and differences in like airframes can play a role in decreasing the accuracy level of coefficient matrices. (1)

Equation (1) is a general algebraic model used to determine the effect of adjustments on helicopter vibrations.

$$[C]_{N \times M} \cdot [Adj]_{M \times 1} = [\Delta Vib]_{N \times 1} \quad (1)$$

The matrix  $[C]$  is the sensitivity coefficient matrix that is specific to a particular type and series helicopter.  $[Adj]$  is the adjustments made, and  $[\Delta Vib]$  is the change in vibrations based on the adjustments made.  $N$  represents the number of specific flight regimes which the data is collected, and  $M$  is the number of adjustment types. (3) In the case of the AH-

64D Apache tail rotor maintenance test, there is only one flight regime and one type of adjustment capability, weight addition and/or subtraction. Equation (1) is still applicable with each blade having a specific sensitivity coefficient. The scalar  $M$  can now represent the number of blades. In order to determine the coefficients  $[C]$ , multiple test sets were created on three to four different Apaches. By making known weight additions or subtractions, then run the measurement analysis again, finally, calculate the change in magnitude and phase per gram of weight. This technique is completed several times for different weight magnitudes on several aircraft to develop an average coefficient for moves on each blade. For each completed adjustment, the sensitivity coefficient matrix  $[C]$  matrix is determined by Equation (2), and then the root-mean-square is calculated to develop an average sensitivity coefficient for moves on each blade. (3)

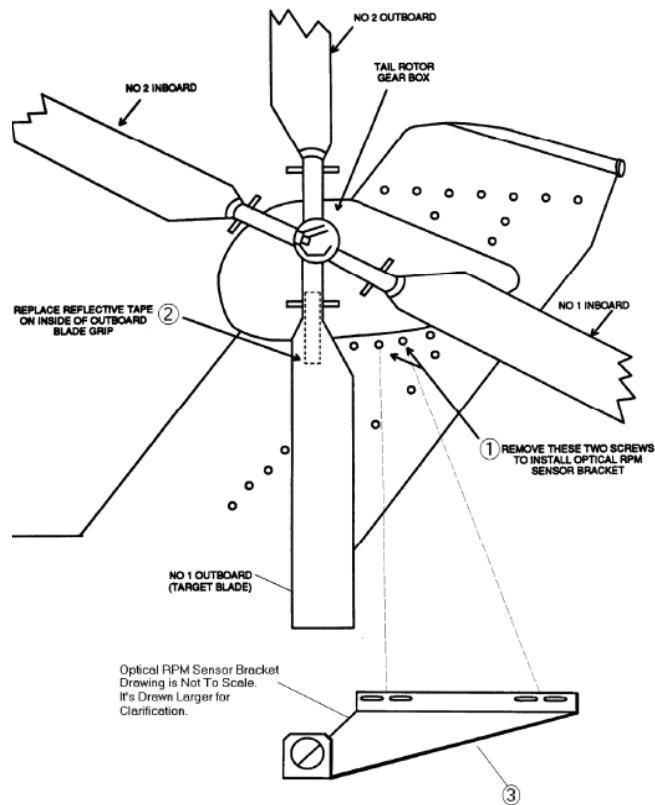
$$C_{nm} = \frac{Vib_{after_n} - Vib_{before_n}}{Adj_m} \quad (2)$$

### **Apache Tail Rotor Vibration Analysis Procedure**

The Army uses a Technical Manual called “Test Set, Aviation Vibration Analyzer” (17) to guide a technician on the proper installation and operation procedures. This manual covers the procedures used on all the helicopters in the Army’s inventory that utilize the AVA for vibration analysis. Since the tail rotor system is identical for the AH-64A Apache and the AH-64D Longbow Apache, the same tail rotor balancing procedures are used. This manual breaks down the tail rotor balancing procedure into six different steps.

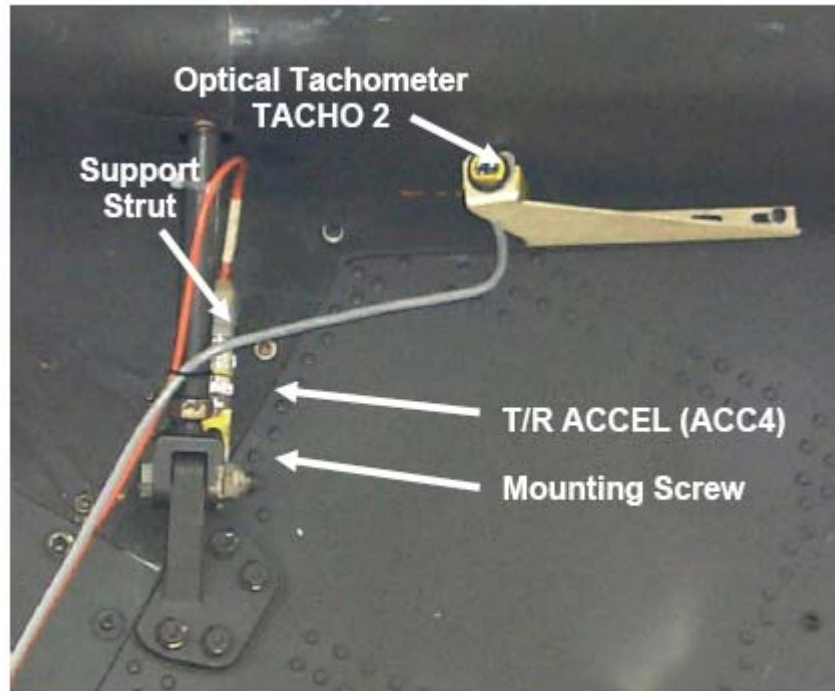
The first step is to remove the AVA tail rotor balancing equipment from its case and inspect it for damage and corrosion to the equipment and cables. Next, the technician hooks up the Data Acquisition Unit (DAU) to the aircraft and connects the Control and Display Unit (CADU) to the DAU.

Figure 4 shows the second step involving the installation of the optical RPM sensor. First, one removes two airframe screws located on the bottom and in the center of the tail rotor gearbox. Next, the technician mounts and secures the sensor bracket to the airframe and then mounts the optical sensor to the bracket. Connect the cable to the rpm sensor and route it down the tail and forward to the DAU. An 8 inch strip of reflective tape is placed on either outboard blade, centered in the spanwise direction. The blade with the reflective tape will be referred to as the No. 1 outboard blade. When looking directly at the hub, the blades rotate in the clock-wise direction. The next blade that passes the rpm sensor is identified as the No. 1 inboard blade. Figure 4 depicts the blade locations and the rpm sensor mounting location.



**Figure 4. RPM Sensor Installation (17)**

In the third step, the accelerometer is installed as shown in Figure 5. The accelerometer is mounted to the accelerometer mounting bracket. The bracket is then mounted to the tail pylon and oriented so the accelerometer is vertical. Connect the accelerometer cable to the accelerometer and route the cables alongside the rpm sensor cable. Finally, connect the wire to the DAU. Figure 5 shows the locations of both the accelerometer and the tachometer



**Figure 5. Accelerometer and Tachometer Installation locations. (17)**

The actual data is collected in step four. The measurement is performed with the pedals centered, the main rotor speed set to 100% (101% for the AH-64D), and the collective is in the full down position, indicating a flat pitch on the main rotor. When the aircraft is steady, the operator initiates the measurement. When the measurement has been successfully acquired, the AVA will automatically proceed to the next screen, and the diagnostics can be displayed.

Step five deals with the diagnostics of the measurements. The tail rotor balance limits are analyzed, if the vibration magnitude exceeds the 0.1 ips limitation, then weight adjustments need to be made in order to lower the amplitude. The manual also states, without explanation, that a weight change to an outboard blade is 50% more effective than an equal weight change to an inboard blade. Based on this statement, the manual is



identifying a relationship based on the inboard blades and outboard blades. Basically, it identifies the outboard blades as being more sensitive compared to the inboard blades.

The AVA will then calculate an adjustment by using the non-learning algorithm method stated earlier in the tail rotor balancing section. Currently, a technician takes the adjustment information, applies the weight adjustments, runs the vibration analysis again, and the amplitude should be within the limitations. On helicopters where the tail rotor blades are 90 degrees apart there is little variation between the coefficients per blade in comparison to the coefficients on the Apache with blades 55 degrees and 125 degrees apart. (12)

The final step in the process is to repeat the measurement and determine whether the corrections had the desired effect. The measurements and adjustments are repeated until the vibration is within the 0.1 ips limitation. (17)

### **III. Methodology**

#### **Rotorcraft Comprehensive Analysis System (RCAS)**

The program used to model the Apache tail rotor system is the Rotorcraft Comprehensive Analysis System (RCAS), an advanced computational analysis program for rotorcraft. This program was originally designed by both the U.S. Army Aeroflight-dynamics Directorate (AFDD) and the Advanced Rotorcraft Technology, Inc (ART) to establish a standard for the helicopter industry to research, engineer, and design helicopters. The program has assisted in improving helicopters that are currently in production along with providing a comprehensive analysis of structural dynamics, aeroelastic stability, vibration, stability and control, performance and loads, and flight dynamics before a prototype is created.

#### **RCAS Coordinate Systems**

The coordinate systems involved in RCAS all follow the right hand rule. Figure 6 identifies an Inertial (I) frame, Global (G) frame, Rigid Body, Hub, and Element frame of reference. The Apache tail rotor RCAS model is primarily represented in the G frame and the Element frame. The initial frame is the inertial coordinate frame. The Z axis is pointing down into the earth, the x axis pointing North and the Y axis pointing East. The RCAS structural model is primarily based on the G (global) frame origin, where the Z-axis is pointing down, the positive X-axis is pointing towards the nose, and the Y-axis is pointing out the right side of the helicopter.

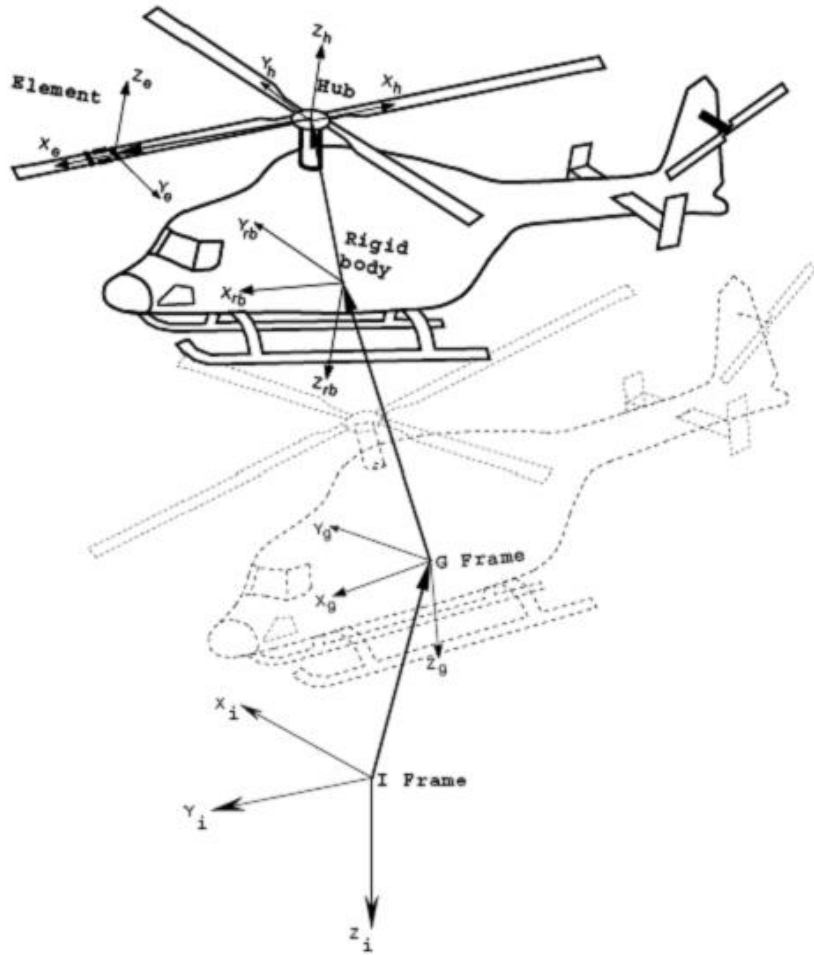


**Figure 6. RCAS Coordinate System's Schematic (6)**

### **Physical Model**

RCAS is architecturally designed in a hierarchical structure. Figure 7 identifies the different physical levels of the RCAS model. The Apache tail rotor model was built from the top down, where the physical model was first identified then the subsequent models were branched off of the top level model. The top level model is composed of a control system, engine/drivetrain, structural and aerodynamic models, however a top level model can exist if one or more of the models are not represented.

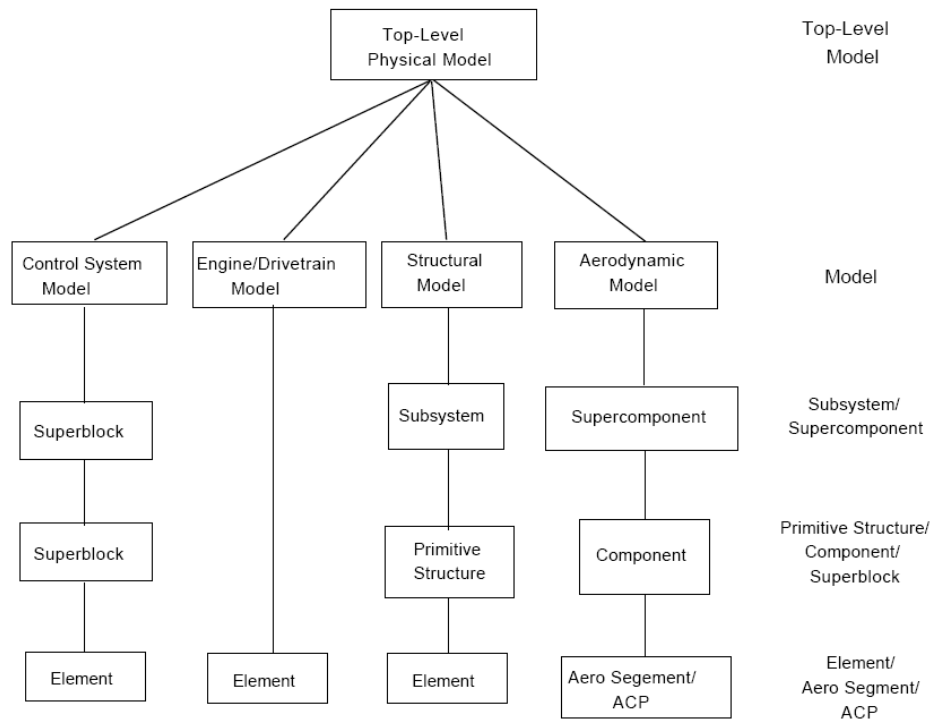


**Figure 7. Block Diagram of the Physical Model (6)**

## Structural Model

The structural model, shown in Figure 8, is a three level hierarchal model consisting of subsystems, primitive structures, and elements. The first step in creating a structural model is to define the coordinate system relative to the reference frame of the model. Similar to the primitive structure, the origin and orientation of the subsystems with respect to the global frame are defined in the SSORIGIN and SSORIENT screens respectively. Each subsystem is comprised of one or more primitive structures, and a primitive structure is a collection of finite elements which are the primary building blocks of the structural model.

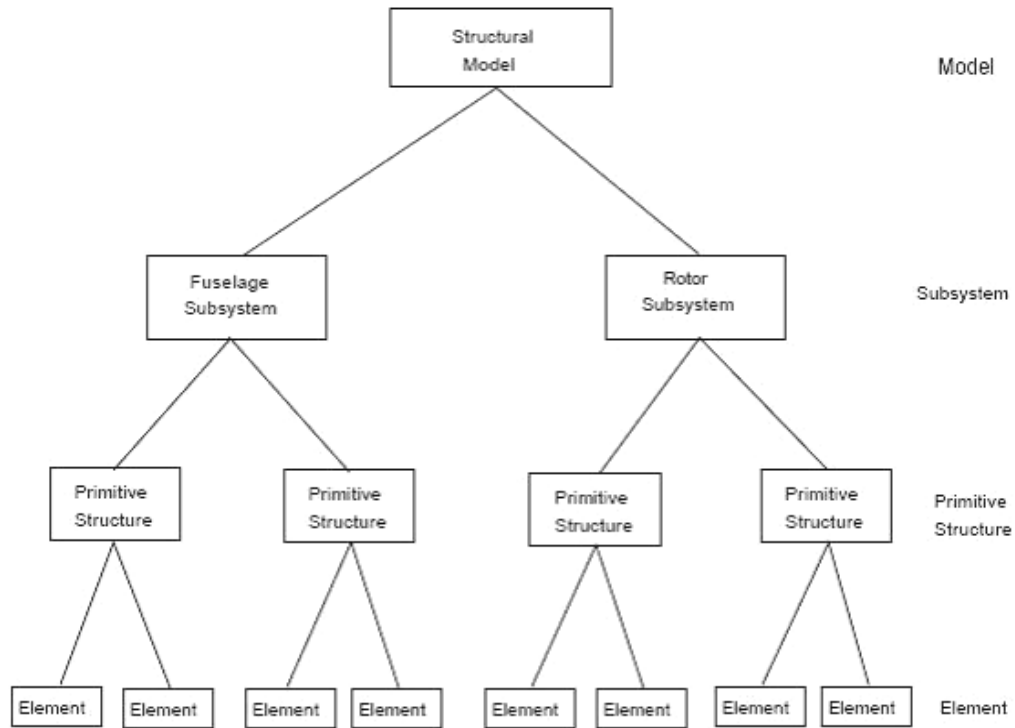


**Figure 8. Block Diagram of the Structural Model (6)**

The structural element is the lowest level of the structural model, and RCAS has 11 types of elements for the user to choose from. The RCAS manual states “A significant (perhaps the most important) effort in the modeling process involves the selection of the element type which most accurately represents that portion of the structural component being modeled.” (6) A structural element has a unique identifier with specific properties and nodal connectivity to the primitive structures. The appropriate elements are selected to best represent the primitive structure; some of the 11 types include springs, dampers, rigid masses, rigid bars, slides, and hinges. Finally, the orientation of an element is the same as the primitive structure in which it is defined.

A primitive structure consists of several structural elements which are arbitrarily connected to each other. The RCAS manual mentions, “The process of creating a finite element model of a primitive structure is perhaps the most involved activity in the model definition process.” (6) The primitive structure is also broken down into geometry dependent and independent data. Geometry dependent data creates the structural geometry of the primitive structure. The geometry dependent data is defined by nodes, elements and connectivities. Geometry independent data consist of physical or mathematical properties that make up the primitive structure’s element, not the location and orientation. All of the primitive structure’s properties are defined in the ELEMPROP menu found within the PRIMSTRUCT menu.

A subsystem can now be created from a collection of primitive structures that represent an independent entity. A subsystem can either be a fuselage, rotor, drivetrain, or control. A structural model can have any number of rotors, but can have only one fuselage, drivetrain, and control. The first step of creating a subsystem is defining the type on the SUBSYSTYP screen. A rotor subsystem is a group of primitive structures, usually labeled as blades, rotating about a fixed point. A fuselage is comprised of one or more primitive structures that are connected together and are fixed. A rotating-to-nonrotating connection ties both a rotor and the fuselage together, this point is also known as the hub node. The parent coordinate system for the primitive structure is defined relative to the coordinate system of the subsystem. The relation between coordinate systems is defined on the PSORIGIN screen and the orientation is defined on the PSORIENT screen. The coordinate system of a rotor must be the hub system H, identified in Figure 6.

## **Aerodynamic Model**

The aerodynamic model has a similar hierarchical structure as the structural model consisting of super-components, components, and aerosegments. A supercomponent is a wing, a rotor, or an aerobody. The supercomponents are a build up of components that are either lifting surfaces or lifting bodies. Multiple aerosegments are the building blocks that make up a component. The aerodynamic forces are computed at specific locations on the aerosegments called Aerodynamic Computation Points (ACP's). The RCAS user's manual describes the multiple calculations performed by the aerodynamic model.

The manual states

“Airloads for rotor blades and other lifting surfaces are based on the lifting line theory and are computed using linear coefficients or table look-up. Corrections for tip loss and yawed flow are available. Linear unsteady effects are computed using the Greenberg Model. Unsteady, nonlinear airfoil dynamic stall effects are represented with the Leishman unsteady aerodynamics model. Inflow may be modeled using the momentum theory, Peters-He finite state dynamic inflow, a prescribed vortex wake, or a free wake. Interference is obtained from the wake of a supercomponent or optional simplified wake interference models.” (6)

Momentum theory is the simplest of the inflow models, external airloads such as wind and gusts, and interference can also be processed into the model in order to create a model that closely mirrors that of reality. The calculation of the airloads requires the local flow velocity at each specific ACP. The velocity is a function of both the rigid body motion and the dynamic response of the structure. A finite element solution is determined at the node point of each element, therefore the structural model nodes should

be aligned with the ACP's. This will allow the aerodynamic loads and moments to be transferred to the structural node points.

Figure 9 represents a RCAS hierarchal aerodynamic model. The lowest level of the model is an aerodynamic segment which is similar to the element of the structural model. A segment's properties include a surface area, orientation, and aerodynamic characteristics. Each segment contains one ACP where the aerodynamic loads are computed. Multiple segments connected together form the aerodynamic component. An aerodynamic component is similar to the primitive structure. An aerodynamic component is identified on the COMPTYPE screen as being a lifting surface, an aerodynamic body, or an auxiliary rotor. A rotor blade is considered to be a lifting surface. The lifting surface component is a series of adjoining arosegments and their respective ACP's. The ACP is located at the center of the arosegment on the quarter-chord span line, the connecting line for the ACP's is also referred to as the lifting line. The lifting line geometry is defined on the AERONODE and AEROSEG screens. An aerodynamic supercomponent is comprised of one or more aerodynamic components. In the case of a tail rotor, the tail rotor system is the aerodynamic supercomponent and the individual tail rotor blades are represented as aerodynamic components. The highest level of the aerodynamic hierarchy is the aerodynamic model. The model sets the origin and orientation of the aerodynamic model with respect to the g frame of reference. The SCORIGIN and SCORIENT screens provide the location to define the common reference frame of the aerodynamic model with the structural model.



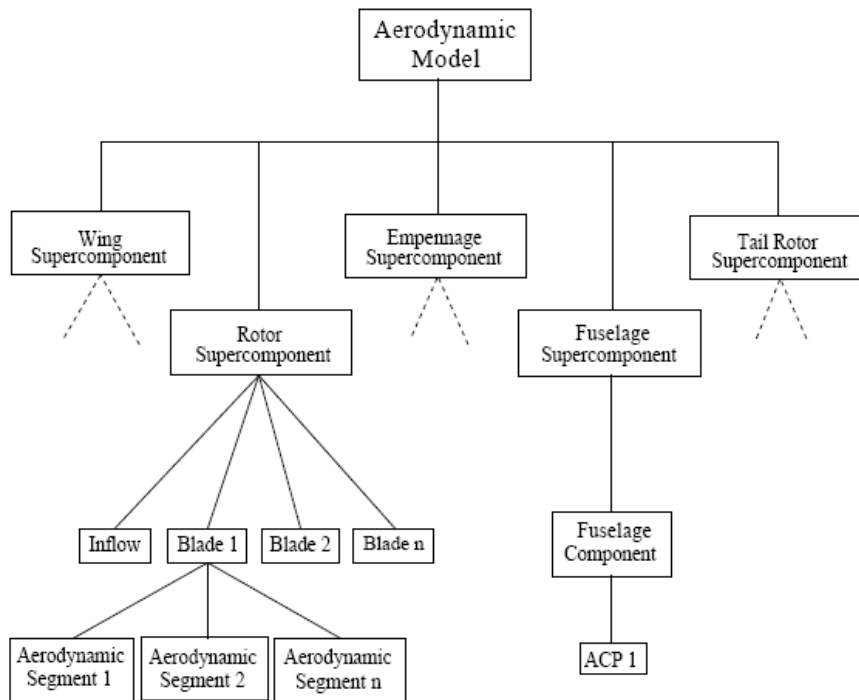


**Figure 9. Aerodynamic Model Hierarchy (6)**

### **AH-64 Apache Tail Rotor Model**

The Apache tail rotor was modeled with only a structural model and aerodynamic model. Appendix A contains the input script code required by RCAS to load the model. Based on the procedures to balance the tail rotor, the controls remain unchanged throughout the testing process; therefore a control system is not required in the model. The tail rotor of the Apache is driven by the main transmission. However; to ensure minimal interference, the engine drive train is not included in the analysis. By eliminating both the main transmission and control system models from the overall physical model, the load effects of the 55 degree phase angle and out-of-plane tail rotor will be isolated.

## AH-64D Structural Model

Figure 10 is a representation of the AH-64 Apache tail rotor's Structural model. Each level of the model will be examined individually and the attributes in which they contain. The subsystems consist of the fuselage (FUSE), the inner tail rotor (TROTORI) and the outer tail rotor (TROTORO). It is imperative that each subsystem is located in the right location with respect to their orientation. The screen GFRAMEORIG in RCAS identifies the G frame origin and the active degrees of freedom. The fuselage is defined as the origin for the tail rotor model. The RCAS computer model requires a minimum of three active degrees of freedom in the G frame. In the case of the Apache tail rotor balancing model, there are three degrees of freedom that need to be addressed in order to find the aircraft's equilibrium. The degrees of freedom are the vertical represented by the translational Z axis, the longitudinal represented by the translational X axis, and finally the yaw is represented by the rotational Z axis.

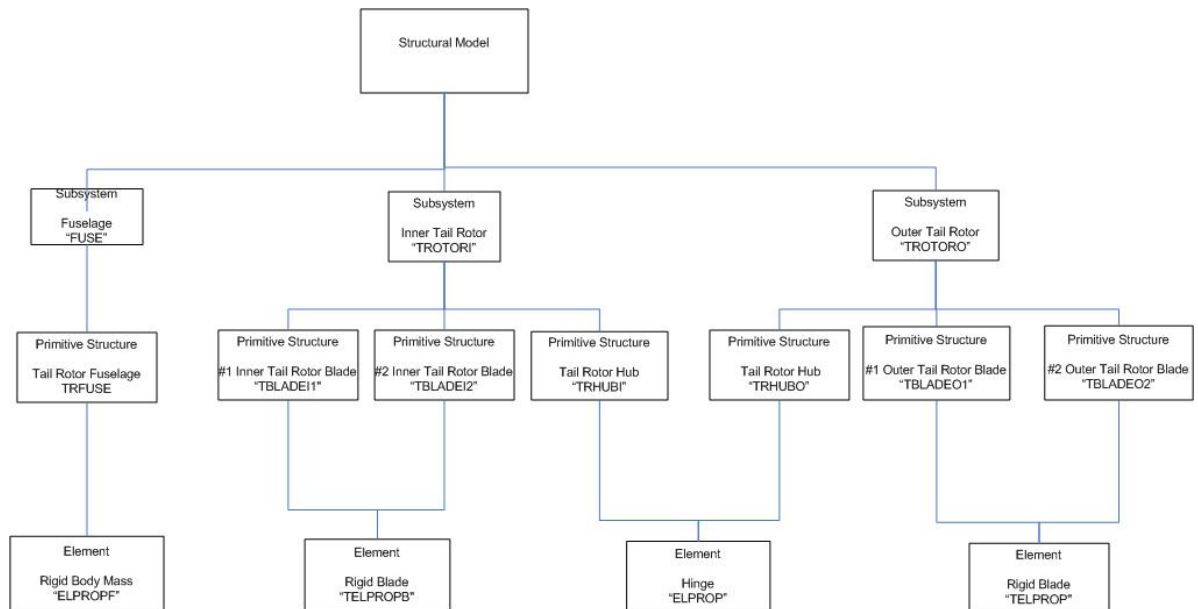


**Figure 10. Apache Structural Model**

The screen SSORIGIN defines the origin of the subsystem with respect to the G frame of reference identified in Figure 6. The FUSE subsystem is located at the origin of the G frame of reference. TROTORI is located 2.47 feet away from the origin, in the negative Y direction. This length accounts for the tail rotor driveshaft from the center of the fuselage to the inner tail rotor. The outer tail rotor is offset 2.96 feet away from the center of the fuselage, allowing for each rotor to respond independently while rotating at the exact rpm. Both tail rotors are offset in the X direction by one foot. This allows the tail rotor hub, to generate a moment about the origin. The thrust, represented at the hub is the amount of thrust generated by the tail to maintain a trimmed balance with the main rotor system.

The screen SSORIENT defines the subsystems orientation with respect to the G frame of reference. Figure 11 shows the rotational sequence of the orientation of both TROTORI and TROTORO. Now the positive Z axis is pointing to the right of the helicopter, the X axis is pointing towards the back and the Y axis is pointing down. In order to better understand the orientation, thrust from the tail rotor subsystem is going to be in the negative Z direction.

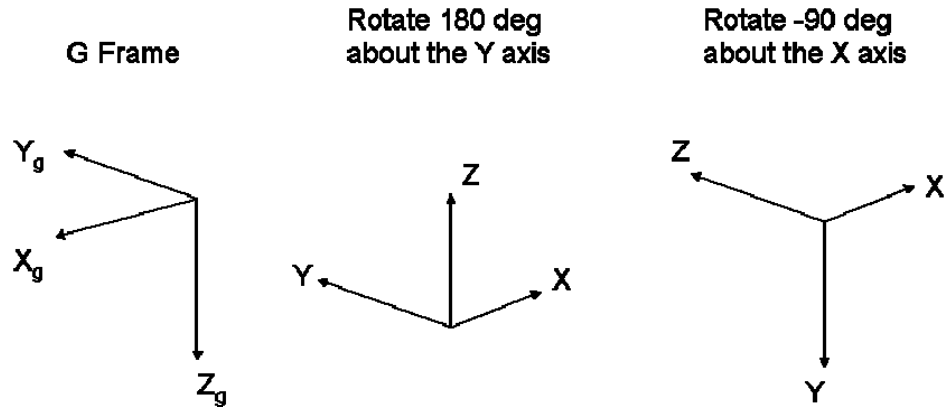


**Figure 11. Rotational Sequence of the Tail Rotor Subsystem**

The CONTROLMIXER screen, located at the bottom of the first page in Appendix A, defines the interface between the pilot inputs and the control surfaces. Trim position inputs can now be entered in degrees and the control mixer conversion factor will affect the control surface in radians as per the RCAS model requirement.

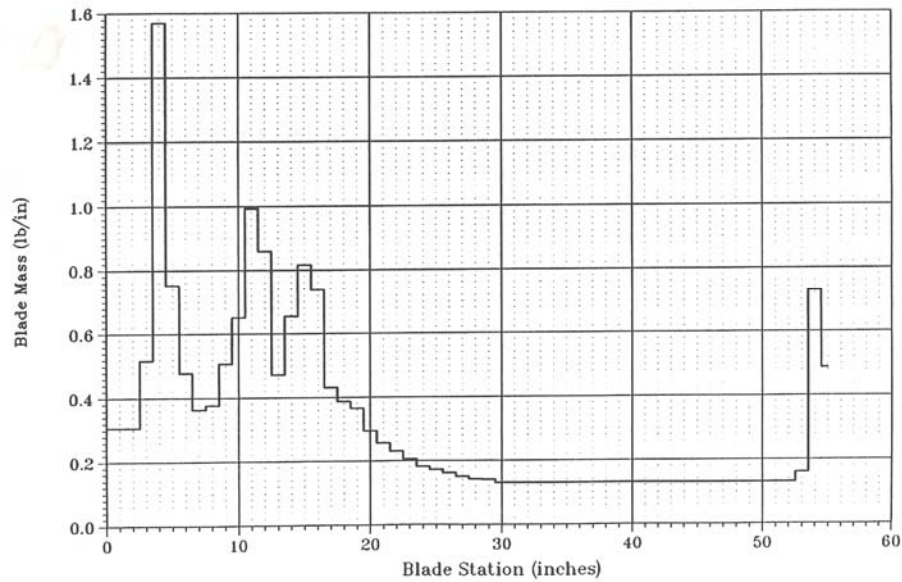
The Apache tail rotor model consists of two rotating subsystems, TROTORI and TROTORO and one non rotating subsystem FUSE. These subsystems are connected in the ROTNONCONST screen. The Fuselage subsystem, FUSE is defined as a nonrotating subsystem and consists of only one primitive structure (TRFUSE). TRFUSE is oriented in the same direction as the fuselage itself. The TRFUSE contains the element properties represented in the element "ELPROP". The Property ID #1 is identified as a rigid body mass with a value close to zero. The RCAS model requires a mass value and in order to ensure minimum interference with the model the fuselage was given a negligible value.

TROTORI is designated as a rotating subsystem consisting of 2 primitive structures, 2 inner tail rotor blades (TBLADEI1 and TBLADEI2), and an inner tail rotor

hub (TRHUBI). All three primitive structures are located at the origin of TROTORI. The primary structure orientation screen, PSORIENT provides the phase location of each blade rotated about the Z axis. The inner blades are located at the -55 degree and -235 degree position on the X-Y plane. TRHUBI is also located at the center of TROTORI to model the fact that the Apache tail rotor system is comprised of two teetering blades. TRHUBI is a mass less structure; therefore its elemental property ID is #1 which has been defined as a negligible mass in order to meet the RCAS requirement that every primitive structure should have a mass. The screen, HINGE, recognizes TRHUBI as a hinge and as a free hinge with zero spring of damping properties about the local Y axis.

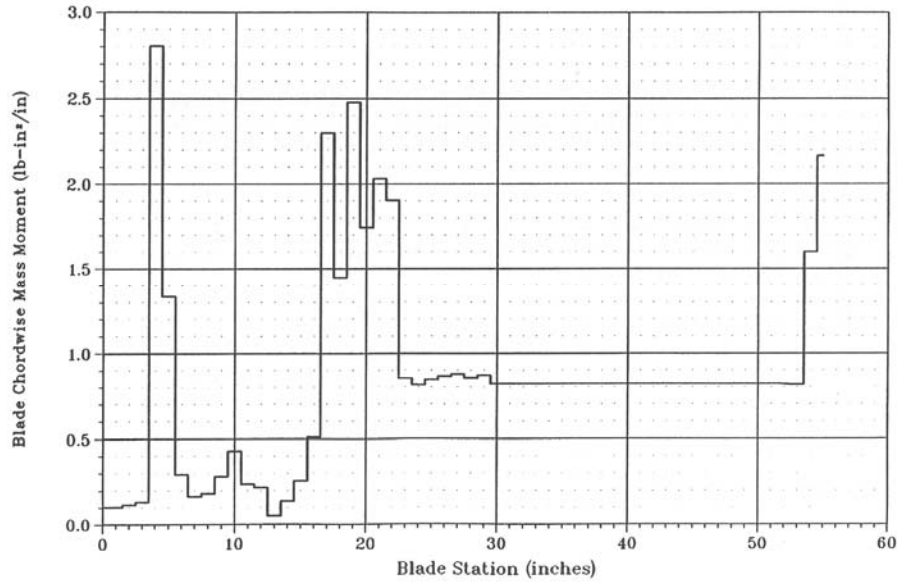
TBLADEI1 and TBLADEI2 are defined as rigid blades, each with a length of 4.58ft. The blades are collectively controlled similar to a swashplate where all blades will move simultaneously in pitch. The elemental properties of the inner tail rotor blade are represented by the element property ELPROP #2. A rigid blade element can contain properties, such as lead lag hinge properties, blade flap hinge properties, pitch bearing properties and element property data (mass, cg, and mass moments of inertia). Only the element property data is required for identifying the Apache's tail rotor blades. Each tail rotor blade has one stainless steel spar and two aluminum spars. Doublers and rivets attach the blade to the blade root, creating a semi-rigid blade system. Due to the minimum effects on the overall internal loads of the tail rotor while it is on the ground, the system is considered to be rigid; therefore the lead-lag and flap hinge properties do not exist. Figure 12 is the mass distribution for the Apache tail rotor. The total mass for each individual blade is 0.58 slugs.

The center of gravity is calculated by multiplying each weight segment by its distance from the root of the blade; those values were then summed and divided by the overall weight of the blade to determine the location of the center of gravity. Based on the data provided from Figure 12, the center of gravity is located at 1.67875 ft. from the origin.



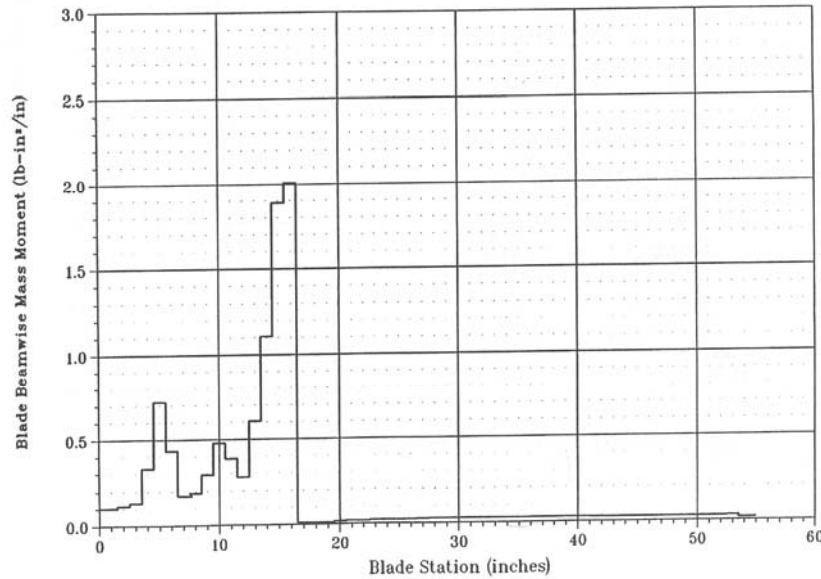
**Figure 12. Apache Tail Rotor Blade Mass Distribution (8)**

Figure 13 displays the tail rotor blade's chordwise mass moment distribution. The feathering moment is the chordwise moment calculated in slugs-ft<sup>2</sup>.  $I_{xx}$ , located on page nine of Appendix A, represents the feathering moment of inertia of the tail rotor blade. The moment is calculated about the longitudinal axis and in the case of the Apache tail rotor, the longitudinal axis runs down the length of the blade at 3.406 inches aft of the leading edge. Thus the feathering moment of inertia about the longitudinal axis is .008903 slugs-ft<sup>2</sup>.



**Figure 13. Apache Tail Rotor Blade Chordwise Mass Moment Distribution (8)**

$I_{yy}$ , also located on the ninth page of Appendix A, represents the flapping moment of inertia, or beamwise moment of inertia of the tail rotor blade about the center of gravity of the blade.  $I_{yy}$  is calculated by using the mass information provided in Figure 12. Each segmented mass is multiplied by the squared value of its distance to the center of gravity (1.67875 ft), and all of the segments are then summed up to equal 1.0069 slugs-ft<sup>2</sup>. In order to ensure an accurate value for  $I_{yy}$ , the beamwise mass moment of each segment should be included in the overall total. Figure 14 is the beamwise mass moment distribution of the Apache tail rotor. The mass moment values for each blade station were converted into feet and added to the previous value of 1.0069 slugs-ft<sup>2</sup>, thus the total value for the flapping moment of inertia is 1.009 slugs-ft<sup>2</sup>.



**Figure 14. Apache Tail Rotor Blade Beamwise Mass Moment Distribution (8)**

Three properties are defined in The element property data set on the ninth page in appendix A has a total of three property identification numbers. The first property ID, #1 is a massless total that was used to add the tail rotor hub and fuselage primitive structures without adding a mass to the overall system. The second property ID, #2, represents the mass of each blade. The third property ID, #3, was developed to adjust the mass of a blade in order to create an imbalanced rotor system.

## Thrust

Thrust from the tail rotor is defined as the amount of force, normal to the main rotor thrust, required to prevent an angular velocity of the helicopter. In order to calculate the tail rotor thrust, the main rotor power and torque must be calculated. Equations 3 and 4 are used to determine the thrust of the tail rotor. When the Apache is on the ground, the main rotor is rotating at 100%  $N_r$  (main rotor rotation speed) for the

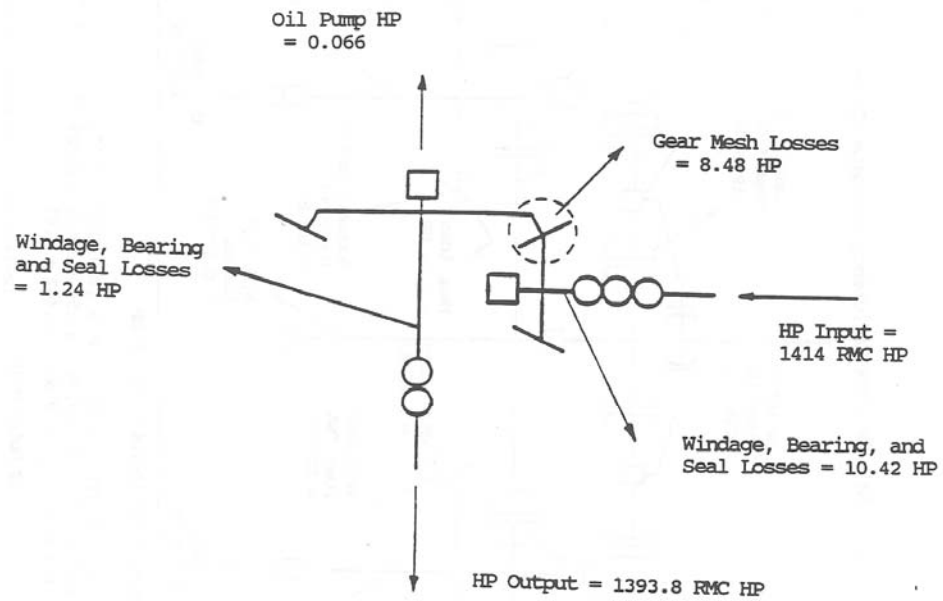


AH-64A Apache or 101% for the AH-64D Longbow Apache, and the tail rotor pedals are centered (50%).

$$Q_{MR} = \frac{P_{MR}}{\Omega_{MR}} \quad (3)$$

$$T_{TR} = \frac{Q_{MRidle}}{X_{TR}} \quad (4)$$

The Apache is powered by two T700-GE-701C engines. Each engine produces 1414 hp. Figure 15 represents the efficiency of the engine nose gearbox. The total power input from each engine is 1414 hp. The power losses in the nose gearbox include an oil pump, gear mesh, bearing, windage, and seal losses. The power output from the nose gearbox is 1393.8 hp. Figure 16 calculates the total power output to the main rotor factoring in similar losses as the nose gearbox in addition to the tail rotor drive shaft and the accessory section. Thus, the overall power output to the main rotor ( $P_{MR}$ ) is 2255 hp. The main rotor torque ( $Q_{MR}$ ) is calculated by dividing the main rotor power by the rotational speed ( $\Omega_{MR}$ ) in radians per second. The Main rotor's 101%  $N_r$  (normal operating speed for the AH-64D Longbow Apache) value is 292 rev/min, this translates to 30.567 radians/second, and therefore the main rotor torque equals 40,575 ft-lbf. The main rotor torque is dependent on the pitch of either the main or tail rotor blade. During the tail rotor balancing procedure, the pedals remain centered, and the collective full down, therefore the torque will remain constant.



$$\text{Total Power Loss} = 10.42 + 8.48 + 0.066 + 1.24 = 20.21 \text{ HP}$$

$$\text{Available Power @ Output} = 1414 - 20.21 = 1393.8$$

$$\text{Gearbox Efficiency} = (1393.8/1414.0) \times 100\% = 98.6\%$$

**Figure 15. Engine Nose Gearbox Efficiency Estimate (8)**

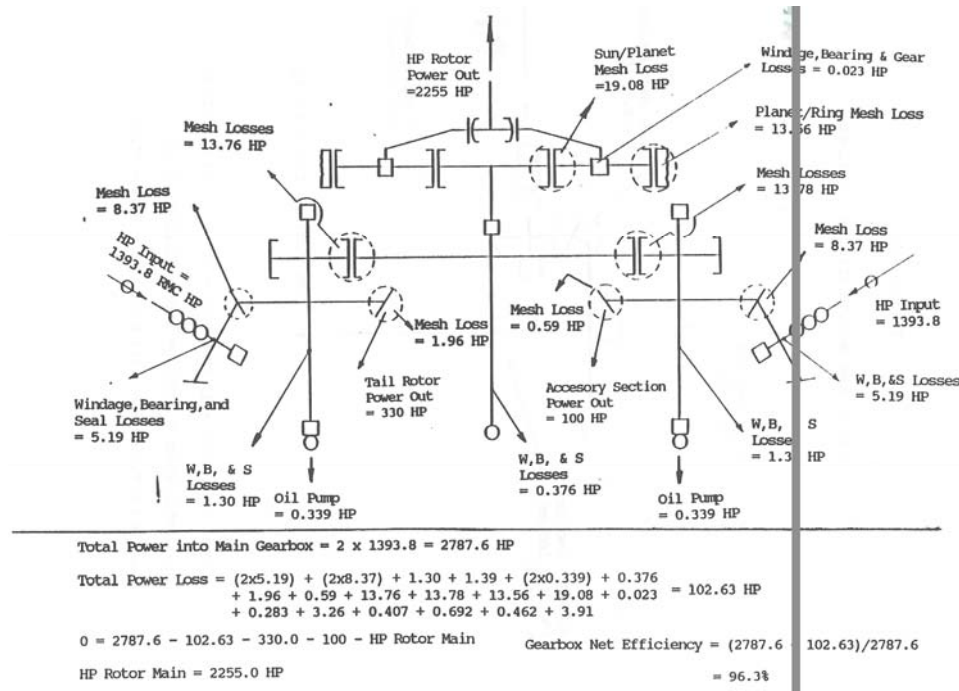


**Figure 16. Main Gearbox Efficiency Estimate (8)**

The hover chart, shown in Figure 17, is used to determine the expected torque required for the Apache to hover out of ground effect (OGE) based on pressure altitude (PA), outside air temperature (OAT), and gross weight. A gross weight of 17000 lbs, a PA of 2500 ft, and a OAT of 15 degrees Celsius were used to calculate the expected torque. Based on these parameters, the expected torque required to hover is 90% of the maximum torque allowed. When the Apache is on deck and the rotational speed is 101%, the torque setting is 6%, therefore the torque of the main rotor at idle ( $Q_{MRidle}$ ) is equal to 2,705 ft-lbf, 6% of the maximum main rotor torque of 40,575 ft-lbf. In order to calculate the thrust needed at the tail rotor, the distance between the main rotor and tail rotor is 29.67 feet. Based on Equation 4, the thrust generated by the Apache tail rotor on the ground with the collective full down, 101%  $N_r$ , is 82 lbf.

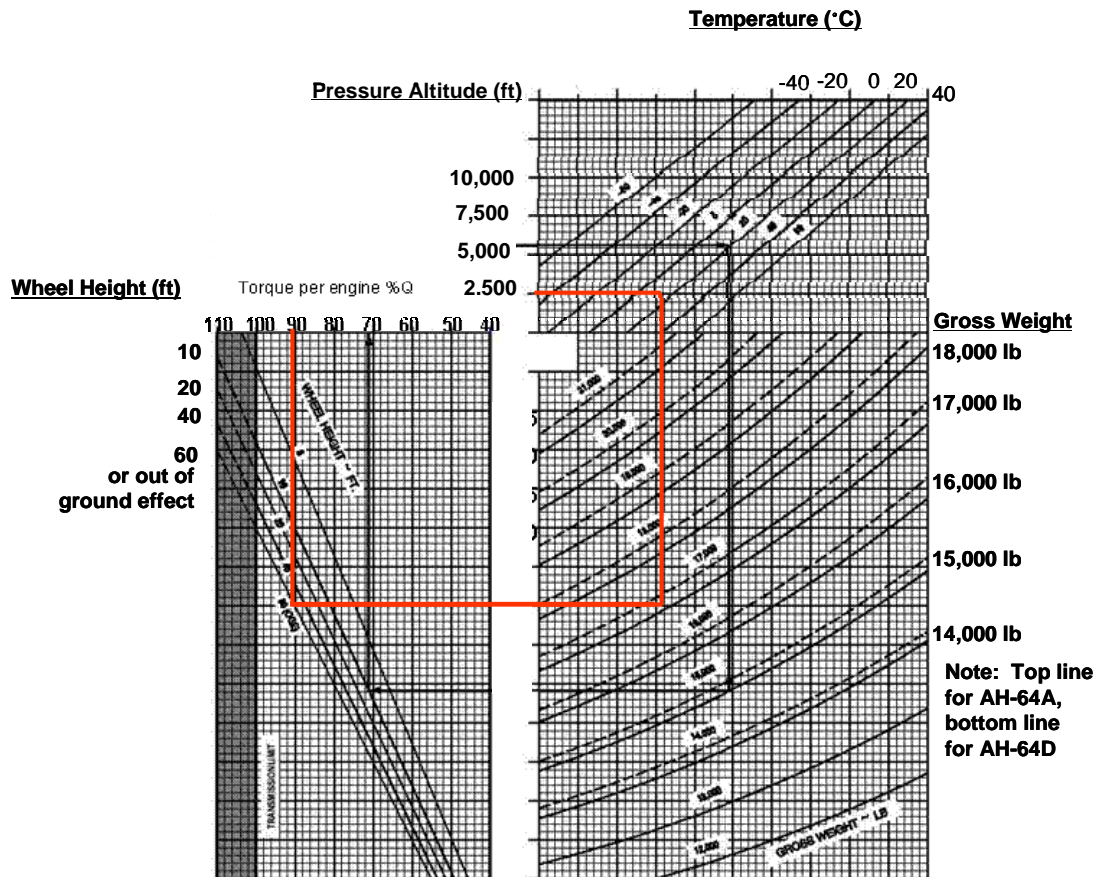
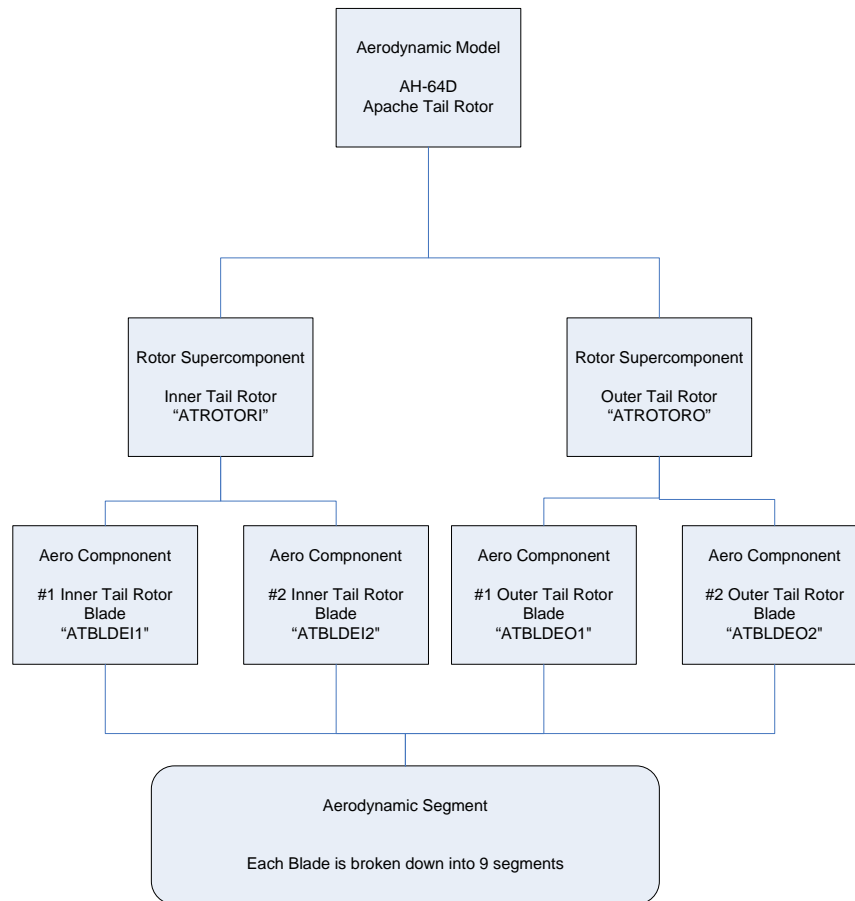


Figure 17. Chart to Determine the Torque Required to Hover (7)

## AH-64D Aerodynamic Model



**Figure 18. AH-64 Apache Tail Rotor Aerodynamic Model**

The aerodynamic model is designed to match the architectural structure of the structural model. The aerodynamic supercomponents are separated into the two rotor subsystems, the inner and outer tail rotor system, similar to the structural model. The origin and orientation of the supercomponents are identical to the structural model, this allows for the aerodynamic forces to be properly aligned with their respective structural subsystem. Both the inner and outer tail rotor aerodynamic supercomponents are offset by one foot in the X direction to create a force that acts at the hub. The inner and outer

tail rotor supercomponents are set out 2.47 and 2.96 feet from the center respectively. This allows for .59 ft of spacing between the two sets of blades. Both aerodynamic supercomponents, ATROTORI and ATROTORO are rotated 180 degrees about the Y axis of the global frame of reference then -90 degrees about the x axis. Figure 11 shows these rotations with respect to the global frame of reference.

The AIRFOIL screen requires the specific airfoil data in the .C81 format. This provides RCAS with a 2 dimensional table of the aerodynamic lift, drag, and pitching coefficients vs. angle of attack and Mach number. This information is then attached to every arosegment where the airfoil ID is specified on the arosegment screen AEROSEG.

The RCAS model accounts for the interference that occurs between the rotors. The RCAS user's manual describes several different types of interference models. Since the analysis is taken when the aircraft is on the ground and the airflow is parallel to the ground, the simple rotor-to rotor interference pertained best for the Apache tail rotor model. According to the RCAS manual, "The interference velocity of this model is estimated from the mean inflow of the interfering rotor, the distance between the two rotors and the overlapping area." (6) After completing runs with and without interference, the result difference is less than ten thousandth of 1% in the outcome in forces. Based on these results, a velocity limit of zero is used for aerodynamic interference.

There are two aerodynamic supercomponents in the RCAS model, ATROTORI and ATROTORO. Each supercomponent consists of 2 aerodynamic blades known as components. There are only two differences between ATROTORO and ATROTORI

supercomponents. The outer blade aerodynamic components are oriented at 0 and 180 degrees on the Z axis, with respect to the supercomponents, and the components inner blades are oriented on the -55 and -235 degree location on the z axis. The other difference is that the ATROTORI supercomponent is associated with the TROTORI subsystem where the ATROTORO supercomponent is coupled with the TROTORO subsystem.

Both supercomponents are modeled as a uniform momentum inflow model. As mentioned in the problem statement, the purpose of researching the tail rotor is to help assist in recognizing predictive trends of the tail rotor, not necessarily specific quantitative values associated with the tail rotor. This is also the reason why higher order aerodynamic modeling options were not selected. The results and conclusions may lead to believe that other models may need to be developed to identify more precise coefficients. According to Leishman, the tip-loss factor accounts for the effective losses in the rotor thrust and induced velocities produced are the blade tips by the trailed vortices. In practice most helicopter rotors have a tip loss value of .95-.98. (5) Tip-loss is a non-dimensional number and tail rotor values are generally lower than main rotors, therefore .95 is used in the Apache RCAS model.

The four aerodynamic components represent the aerodynamic make up of each rotor blade. Each component is a mirror image of the other; therefore only one master component is developed and then copied onto the other three components. The blade is broken down into 10 nodes which create 9 arosegments.

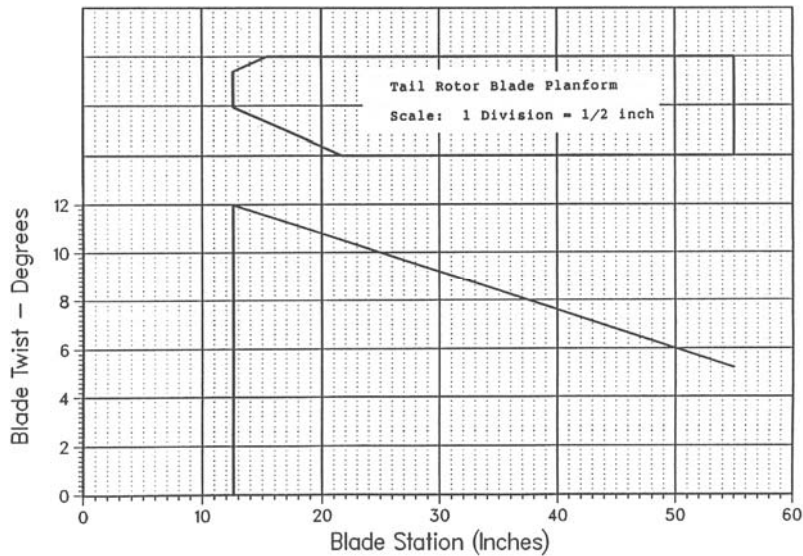


**Figure 19. Longbow Apache Tail Rotor Blade Planform and Twist Distribution (8)**

An aerosegment's properties include chord length, the airfoil ID, TBLADEAF, and a twist radian. Figure 19 shows the chord length and blade twist. The root is tapered for the first 10 inches in length. The tail rotor maintains a constant 10 inch chord from 21 inches to the tip at 55 inches. Figure 19 also identifies the rotor blade twist from the root to the tip. The twist distribution is linear at  $-0.158$  deg/in. and starts at the root from 12 degrees and decreases to 5.2 degrees at the tip. Negative twist, known as washout, is designed to redistribute the lift over the blade and help reduce the induced power, to a point. (5) The airfoil ID TBLADEAF is used to represent every segment of the tail rotor. Again, TBLADEAF uses the NACA 63-414 mod data tables and coefficients in the .C81 file data format.

### Comparative Model and Data Output

An Apache model, where the blades are 90 degrees apart, is used for comparison and validation of the results produced by the more realistic Apache model with the outer



blades at the 0/180 degrees and the inner blades at the 55/235 degree locations. The 90 degree model will be referred to as the “Traditional Model.” The primary difference between the two models is TBLADEI1&2 and TBLADEO1&2 primitive structure orientations to their respective subsystems. It is also imperative to adjust the aerodynamic model’s component orientation with respect to their supercomponent as well.

RCAS provides the data results through a technology output processor (TOP). This processor is capable of processing data analysis of airloads, structural dynamics, internal loads, and many more. In the case of the Apache tail rotor model, the internal loads will be analyzed in multiple scenarios. The scenarios to be looked at will help to validate the models and determine the internal loads of the Apache model both balanced and imbalanced.

The results will focus on the internal loads at the rotor hub. The hub measurement will mirror the real world accelerometer readings by also taking into account the difference in the inner rotor and outer rotor moments on the shaft. When describing the structural model, it was mentioned that the hub was offset 1 ft in order to measure a force. If the model was not offset, then the value of the internal load would have been zero and the internal load data output would not exist. The Apache Rotor Balance section also mentioned that the Accelerometer collects data in the form of g’s and calculates an ips value. Acceleration is known as the rate at which a velocity changes with respect to time. Newton’s Second Law states that force is equal to mass times acceleration. For each run, mass remains constant, therefore the force exerted on the blade is proportional to the acceleration. It is now clear that the force data processed

by the internal load TOP is directly related to the raw data generated from the tail rotor accelerometer.

The problem statement section mentioned that it was possible to add a second accelerometer on the Y axis (lateral). Also if the data collected identifies that it is beneficial to collect data in the X-axis, a new mounting bracket can be designed. In order to analyze all three axes, the internal forces with respect to azimuth for one revolution must be collected in all three axes.

The results of both the Apache RCAS model and 90 degree model will be analyzed in four sets of information. Multiple weights will be added to a single blade, one weight will be added to multiple blades, a combination of equal weights will be added to 2 adjacent blades, and finally 2 unequal weights will be added to adjacent blades.

## IV: Results and Discussion

### Introduction

As mentioned before, weights can be added and removed from two pockets located at the tip of the blade. During the tail rotor balancing procedure, an equal weight adjustment should be made at both locations. Each “weight unit” has a mass of exactly 1 gram, and each blade can hold a total of 60 grams. Common weight adjustments occur between one gram and 20 grams. The weight adjustment for weight set one, located in Table 1 was chosen in order to allow for data points to be a suitable distance away from the origin. Although it is uncommon to have weight adjustments greater than 20 grams, there have been many documented cases where adjustments were greater than 20 grams. The weights listed in Table 1 will be used in multiple combinations and different scenarios in order to simulate various imbalances that can be found with a tail rotor system.

**Table 1**

Weight Set	Grams	Slugs
1	2	.000137044
2	4	.000274087
3	10	.000685219
4	20	.001370437
5	26	.00178156

The charts generated by RCAS display the phase angles in degrees and amplitudes in force (lbf). Phase angles are measured based off of the reference blade, No.1 outer blade. The tail rotor vibration analysis procedures use the outer tail rotor with the reflective tape as their zero degree reference. In the case of the RCAS Apache model, the No.1 outer tail rotor blade has been designated as the reference blade. During the simulations where an imbalance occurs, the phase angle will be measured from the zero azimuth to the azimuth angle where a zero amplitude exists as the wave travels from a negative number to a positive number. Amplitude is simply the maximum displacement from the periodic wave's equilibrium. In the case of the Apache tail rotor model, the equilibrium force in the vertical direction is the weight of the tail rotor. In reality, a mean amplitude is taken into account, however for the theoretical RCAS model, the amplitudes will be the same for every revolution or complete cycle.

All of the charts displaying the forces in the Z direction have a mean amplitude of 74.7 lbf. This value is determined by the overall gravitational weight of the tail rotor system. The charts that have forces in the X direction have a mean amplitude of zero lbf. Finally, the mean amplitude of all charts with forces in Y direction is 82 lbf, or in the case of the Apache, the RCAS input value for thrust.

### **Multiple Weights, Single Blade**

The first set of simulations involved adding different weights to a single blade. All five weight sets were utilized and No.1 inner blade was arbitrarily chosen. When weight is added to a specific blade on a balanced model, the phase angle will occur at the

phase location of that blade. In the case of the traditional model, the No.1 inner blade trails the reference blade, outer No.1 blade, by 90 degrees; therefore the phase angle is expected to be 90 degrees. Figure 20 is a chart created from the traditional model by adding weight to the inner No1. blade and displays the forces in the Z direction with respect to the azimuth. The chart shows the changes in force when multiple weights; 2, 4, 10, 20 and 26 grams are added to a single blade. Note that the phase angle occurs at 90.6 degrees in all five cases, the location of the inner No.1 blade. Figure 20 also displays the increase in forces in the Z direction as the weight is added to the inner No1. blade.

Figure 21 represents the same process described above applied to the Apache model. In the Apache model, the inner No.1 blade trails the reference blade by 55 degrees and when weight is added to this blade, the phase angle is expected to be 55 degrees. The phase angle in Figure 21 occurs at 55.6 degrees, this aligns it with the inner No.1 tail rotor blade. When weight was added to the inner No.1 blade in the Apache model, the amplitude of the force in the Z direction increased as well.

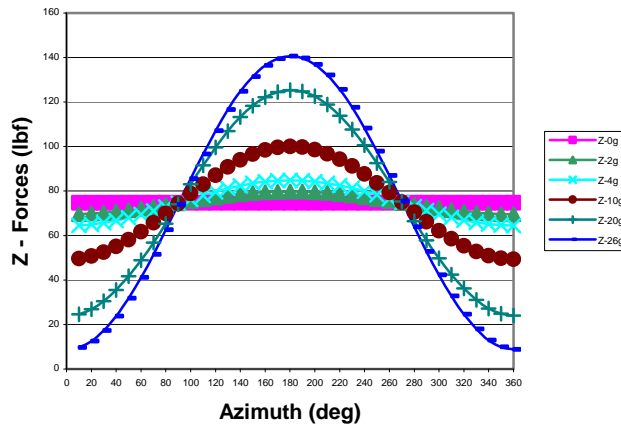


**Figure 20. Traditional – Multiple Weights, Single Blade – Z forces**

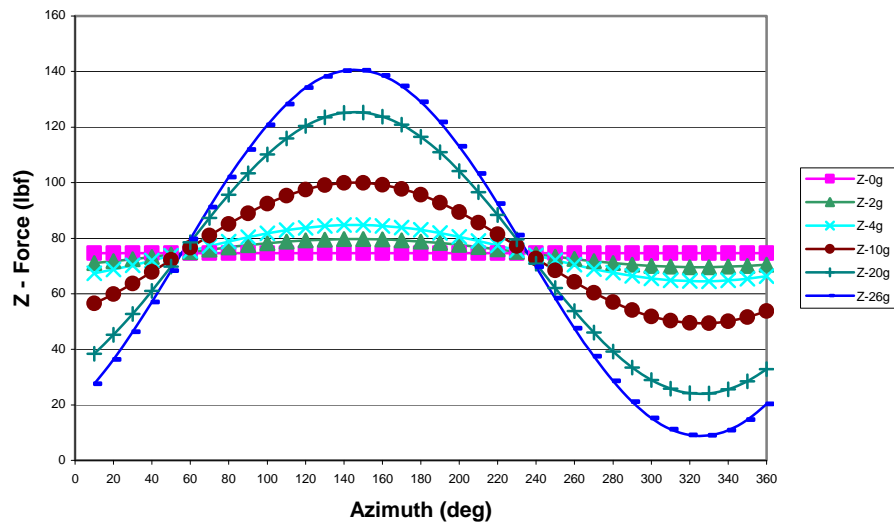


**Figure 21. Apache – Multiple Weights, Single Blade**

The Traditional and Apache models phase angles intersected the mean amplitude approximately 0.5 to 0.6 degrees different from the expected values. There are several factors within the RCAS model that could account for this deviation; some include trim variable tolerances, gravity effects, and aerodynamic effects.

Both charts help validate the models ability to respond correctly to a weight addition to a single blade. When weight was added to the blade, the amplitude increased for both models. The next question to be answered by the single blade, multiple weights simulation is; “Does the increase in weight have a linear effect on the Amplitude?” Figure 22 depicts the relationship between weight added and the increase in amplitude and according to the model, both the Apache and traditional model’s relationship is linear.

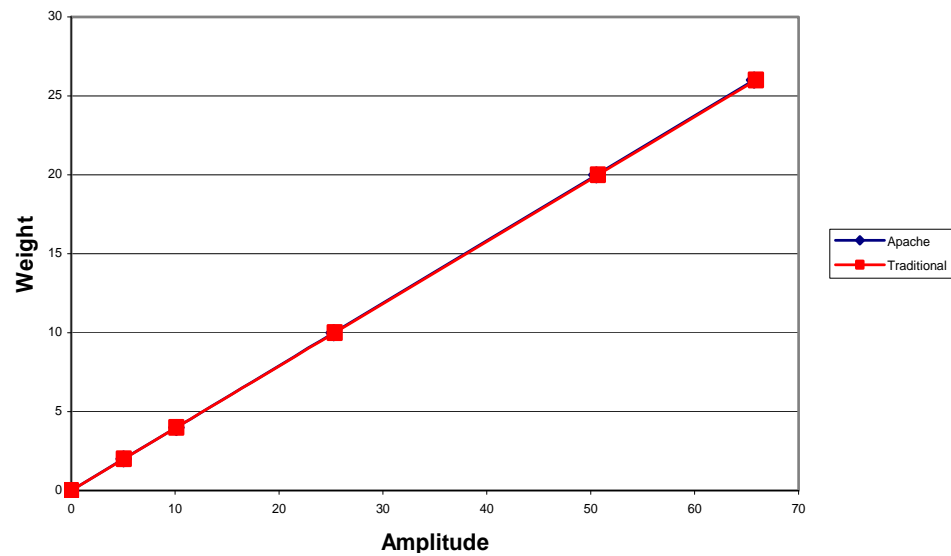


**Figure 22. Weight to Amplitude Relationship, Both Models**

### Single Weight, Multiple Blades

In the first simulation, multiple weights were added to a single blade in both the Apache model and the Traditional model. In both models, the phase angle occurred at the location of the specified blade that had the additional weight. Adding multiple weights to a single blade also identified that the amplitude increases linearly as more weight was added. In this simulation, weight set three (10g) is added to each blade, one blade at a time. In this case, the phase is expected to occur at the location where specific blade with the ten additional grams is oriented, for example, the phase for the No.1 inner blade should be at 55 degrees in the Apache model. The other factor to consider is the amplitude. Since the weight set is equal for all cases, there should not be a variation in amplitude.

Figure 23 depicts the results of running four simulations. In the first simulation, ten grams were added to the outer No.1 tail rotor blade and the results are represented by

the yellow line. In the next simulation, the added 10 grams of weight was removed from the outer No.1 blade and ten grams were placed onto the inner No.1 blade, the results are displayed on the navy blue line in Figure 23. This process continued with the outer No.2 blade and inner No.2 blade. It is evident in Figure 23 that the phase occurs at zero when 10 grams are added to the outer No.1 blade, also known as the reference blade. When 10 grams are added to the inner No.1 blade the phase lies on the 90 degree azimuth, the exact location of the tail rotor blade. The same results occurred at 180, and 270 degrees, with the outer No.2 and inner No.2 blades respectively. It is also noted that the amplitude for all four simulations is 25.3 lbf..

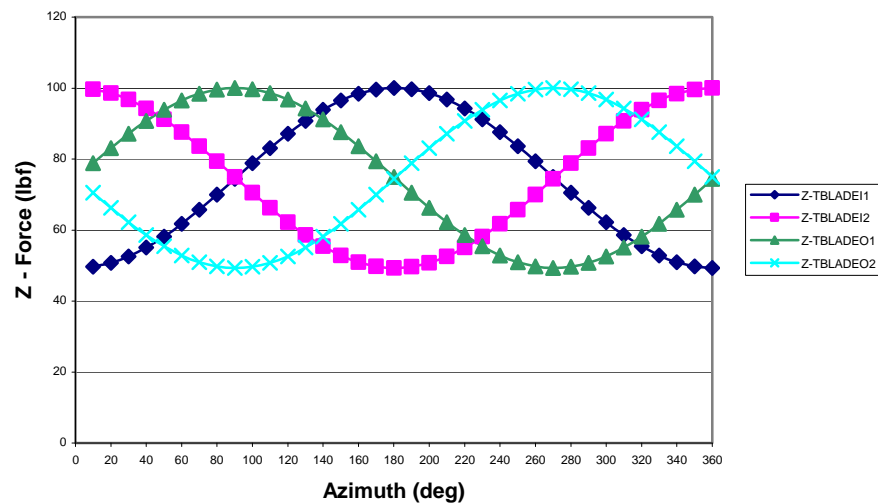


**Figure 23. Traditional – Z force w/ 10g added 1 Blade at a Time**

The exact process was repeated with the Apache model and the results are shown in Figure 24. The phase angle for the outer No.1 blade occurred at zero degrees, the phase angle for the inner No.1 phase occurred at 55 degrees, which is its location with respect to the reference blade, outer No.1. The same held true for the phase angle of the



outer No.2 and inner No.2 blades located at 180 and 235 degrees respectively from the reference blade. The Apache rotor system's amplitude in all four simulations was 25.3 lbf, the same value as the traditional model. Based on the results from the eight simulations, every blade responds as expected to the addition of a set weight amount to each individual blade.

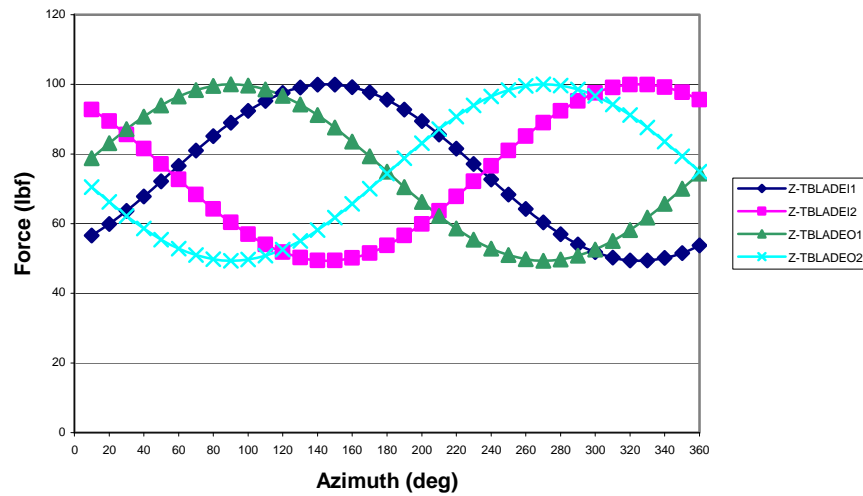


**Figure 24. Apache – Z force w/ 10g added 1 Blade at a Time**

Throughout the simulations, more questions were asked on what could have an effect on the phase and amplitude of the rotor system, one factor in question was thrust. Does thrust have an effect on the phase or amplitude? Figure 25 shows the phase and amplitude of 10g added to the No.1 inner blade for both the Traditional and Apache rotor system model, lines *Traditional Z-TBLADEI1* and *Apache Z-TBLADEI1* respectively. The *Apache Thrust -300lbf* line, in Figure 25, is the Apache rotor system model with 10g added to the No.1 inner blade along with a change of thrust from -82 lbf in the Z

direction to -300 lbf. The chart clearly shows that thrust does not factor into the internal loads on the hub which are used to calculate the phase and amplitude.

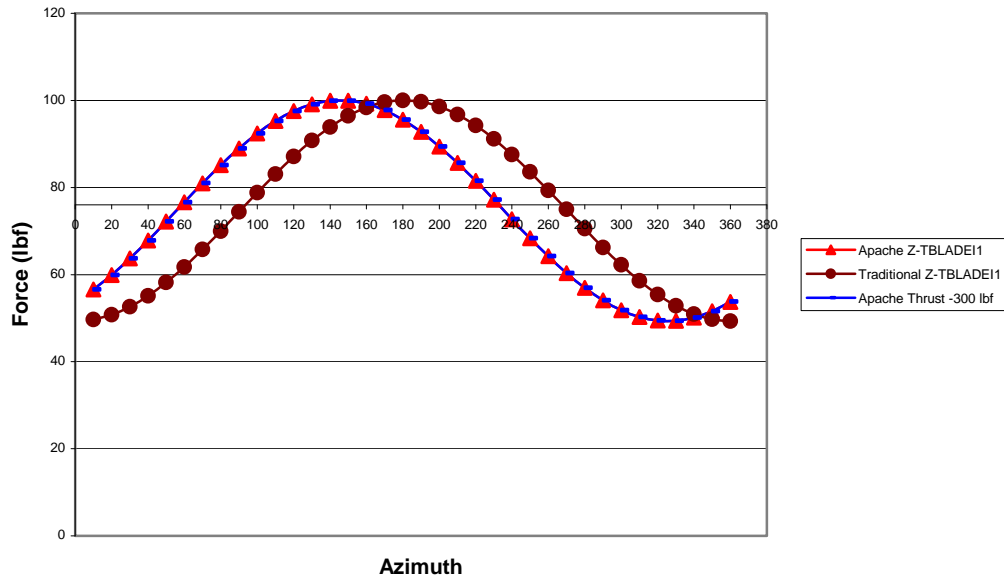
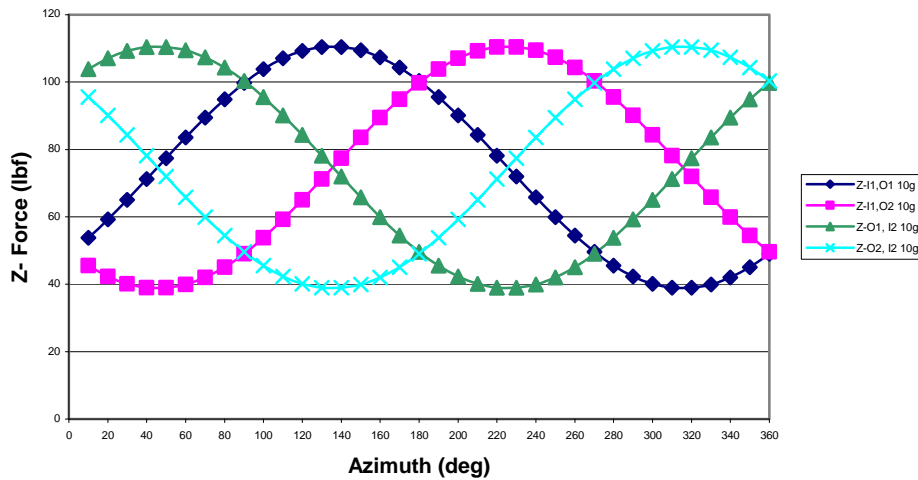


**Figure 25. Z forces on 82 lbf and 300 lbf of Thrust**

### **Equal Weights Added to Adjacent Blades**

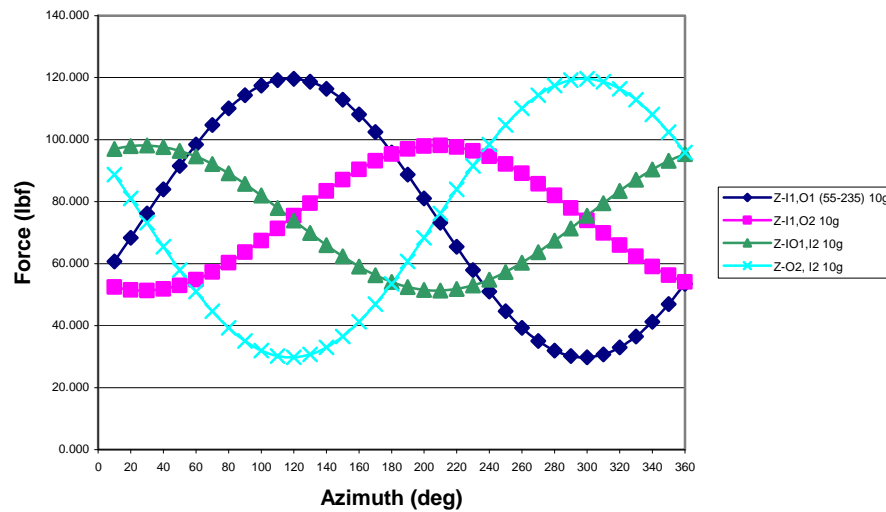
In the third scenario, weight set three (10g) was added to two adjacent blades at a time. The weight combinations included outer and inner No.1 blades, inner No.1 and outer No.2 blades, outer No.2 and inner No.2 blades, and finally the inner No.2 and outer No.1 blades. Based on the previous simulations, it would be expected that the phase would be located exactly half way between the blades which would correspond to the total weight being split between the two blades. Equal weight is added to each adjacent blade; as a result it is expected that the amplitude of force in the Z-direction should be the same in all four scenarios

Figure 26 shows the results from the simulations performed based on the four scenarios described above using the traditional model. In the legend, Figure 26 and all the following figures, Z represents the force direction, “I” or “O” distinguishes between the inner or outer blade respectively, “1” or “2” identifies the blade number, and finally the last value is the weight added to the blade(s). The phase angle was 45 degrees when the weight was added to the inner and outer No.1 rotor blades labeled *Z-II,O1 10g*, 135 degrees for the Inner No.1 and Outer No.2 blades labeled *Z-II,O2 10g*, 225 degrees for the outer No.2 and inner No.2 blades labeled *Z-O2, I2 10g*, and 315 degrees for the inner No.2 and outer No.1 blades labeled *Z-O1, I2 10g*. All four scenarios showed that the phase angle was located exactly half way between the adjacent blades where weight was added. The amplitude of the force in the Z direction, as expected, was the same for all four scenarios, 35.75 lbf.



**Figure 26. Traditional Equal wt (10g) to Adjacent Blades**

When the weights were distributed between two adjacent blades in the Apache model, the phase results were similar to the traditional model where all the phase angles were aligned to the center of the quadrant that was bounded by two blades with weight additions. The amplitudes represented by force in the Z direction were not equal in the four scenarios. When the two 55 degree quadrants were bounded by blades with additional weight, the amplitudes were 44.98 lbf and when the 125 degree quadrants were surrounded by blades that had the weight addition, the amplitude was 23.38 lbf. These results show an increase in amplitude of 92.4% when comparing the 125-degree quadrants to the 55-degree quadrants.



**Figure 27. Apache Equal wt (10g) to Adjacent Blades**

### **Unequal Weights, Adjacent Blades**

The final simulations consisted of adding unequal amounts of weight to adjacent blades. Again, four scenarios were simulated. The weight combinations included four grams on the outer and ten grams on the inner No.1 blades, ten grams on the inner No.1 and four grams on the outer No.2 blades, four grams on the inner No.2 and ten grams on the outer No.1 blades, and finally ten grams on the outer No.2 and four grams on the inner No.2 blades. The results of the four scenarios applied to the traditional model are shown in Figure 28. In this simulation, the phase appears to be located closer to the blade with the heavier weight. For example, in the first scenario the phase angle is 68.8 degrees. This is only 21.2 degrees away from the Inner No.1 blade and 68.8 degrees away from the Outer No.1 blade. In the traditional model, the proportion between the phase angle and the size of the quadrant is close to the correct distribution of weight (10 grams and 4 grams) between blades. In this case the difference is approximately 5%. If

most weight adjustments are within 20 grams then most adjustments in the traditional model case would be within one gram. Figure 28 also shows that the amplitude remained the same in all four scenarios.

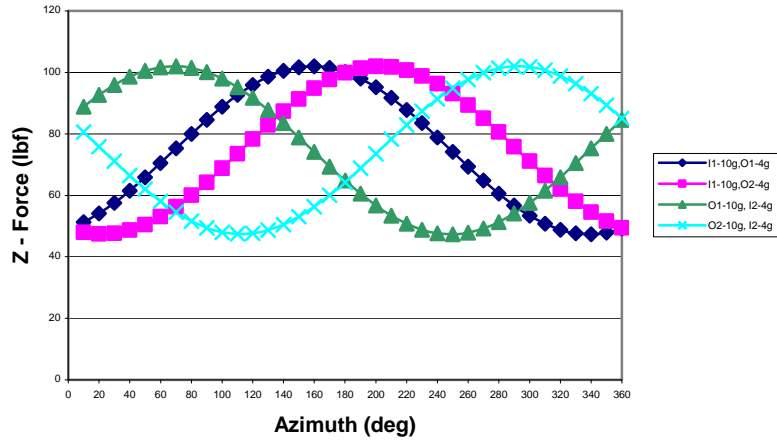


**Figure 28. Traditional Rotor System 10g-4g Adjacent Blades**

The results from the Apache model simulation where the same unequal weight combinations were applied to the same blades are shown in Figure 29. The proportions in the 55 degree and 125 degree quadrants that are split by the phase angle were similar in the Apache model as they were in the traditional model. For example, the phase angle for the first scenario was 40.7 degrees. In this case, 10 grams were added to the inner No.1 blade and 4 grams added to the outer No.1 blade. The difference in the actual proportion and the model's generated phase angle proportion is 3.5%. Again, there is a difference noticed in the amplitudes between the 55-degree quadrants and the 125 degree quadrants. When two blades with weight added bound a 55-degree quadrant, the amplitude is 31.26 lbf, and when the 125 degree quadrants are bounded by two blades with weight is added, the amplitude is 21.56 lbf. In the Apache model simulation

involving unequal weights (ten grams and four grams) the difference in amplitudes is 45.2%, far less than the 92% when the weight distribution was equal. This observation leads to the one to believe that as the difference in weight distribution (proportion split between two blades) increases, the amplitudes approach magnitude of the total weight determined when all the weight is added to one specific blade.

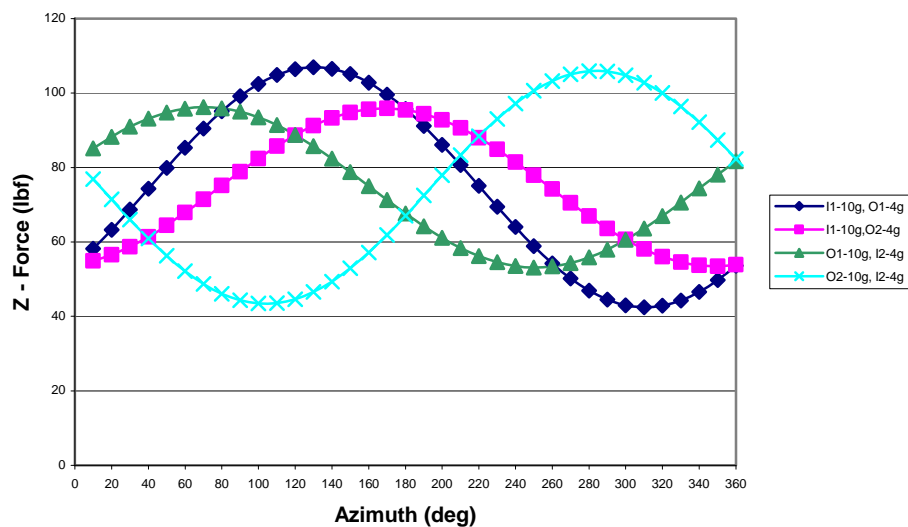


**Figure 29. Apache Rotor System 10g-4g Adjacent Blades**

It was previously mentioned, and it is depicted in Figure 22; as weight is added to a blade, there is a linear relationship between the increase in amplitude and the increase in weight. Figure 30 identifies 4 different linear relationships between weight and amplitude, these relationships are, when multiple weights are added to the No.1 inner blade labeled *No.1 Inner Blade*, the Inner No.1 and outer No.1 blades labeled *Z II-O1 (55)* in the Apache model which create a 55-degree quadrant, the inner No.1 and outer No.2 blades labeled *Z II-O2 (125)* in the Apache model that create a 125-degree quadrant

and the inner and outer No.1 blades labeled *Z II-OI (90)* in the traditional model which represent a 90 degree quadrant. The slope of the line that defines each scenario's total weight with respect to amplitude is different and they are not linearly spaced based on the size of the quadrant.

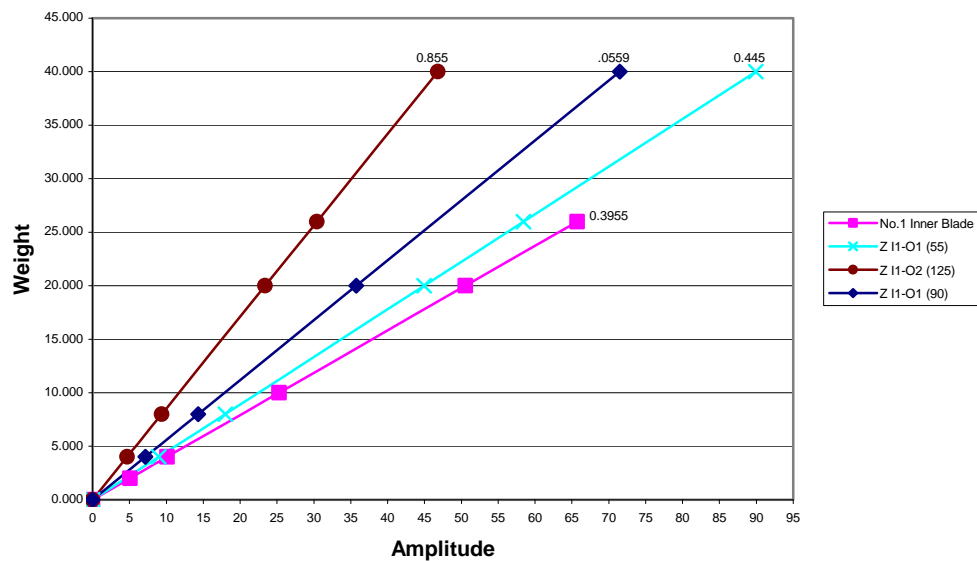


**Figure 30. Multiple Weights Added to No. 1 Inner Blade and the Bounding Blades of 3 Different Quadrant Sizes**

The next step was to analyze the weight to amplitude relationship of multiple weight combinations. The combinations simulated were 2 and 26 grams, 4 and 10 grams, 10 and 20 grams, 20 and 10 grams, 4 and 2 grams, 2 and 4 grams, 10 and 4 grams, 26 and 2 grams. The weight sets can be viewed as 2 sets that are equidistant from each bounded blade. This will help to determine if the distributions within a specific quadrant is symmetric. The two weight sets 10 and 20 grams and 2 and 4 grams are equal



proportions of weight distribution. This will help to verify that if the proportions are the same, regardless of weight, their weight to amplitude line will have the same slope.

The following 3 figures represent the linear relationships between the distribution of weight sets mentioned in the previous paragraph with respect to amplitude. Figure 31 represents the different weight to amplitude distribution using the different weight sets combinations in a 90 degree quadrant. Figure 32 and Figure 33 shows the exact same approach as Figure 31 but using a 55 degree quadrant and 125 degree quadrant respectively.

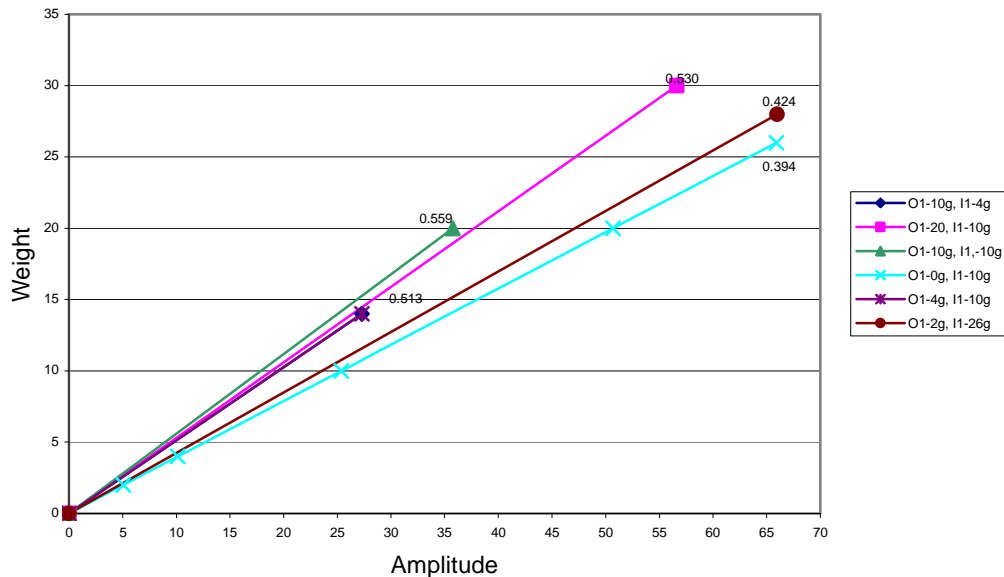


**Figure 31. 90 Degree Quadrant Weight to Amplitude Distribution**

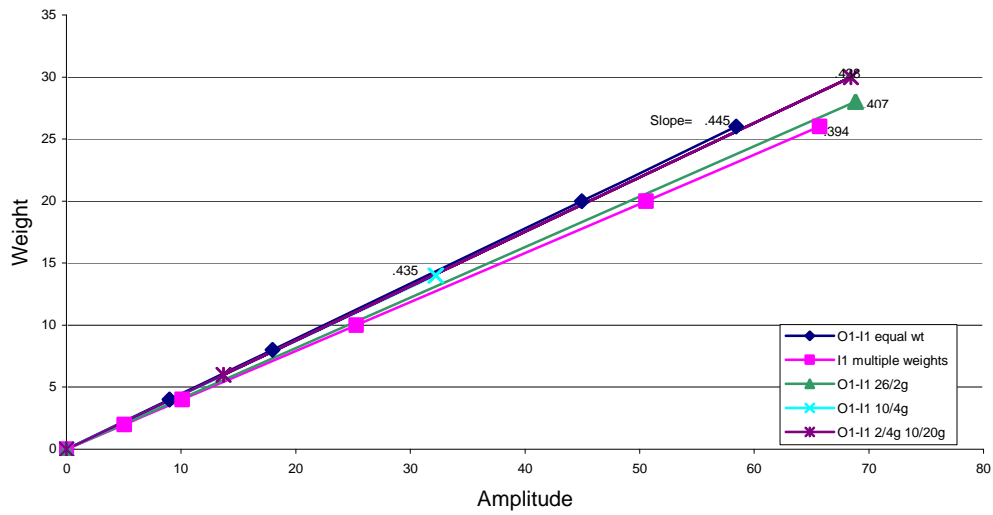


**Figure 32. 55 Degree Quadrant Weight to Amplitude Distribution**

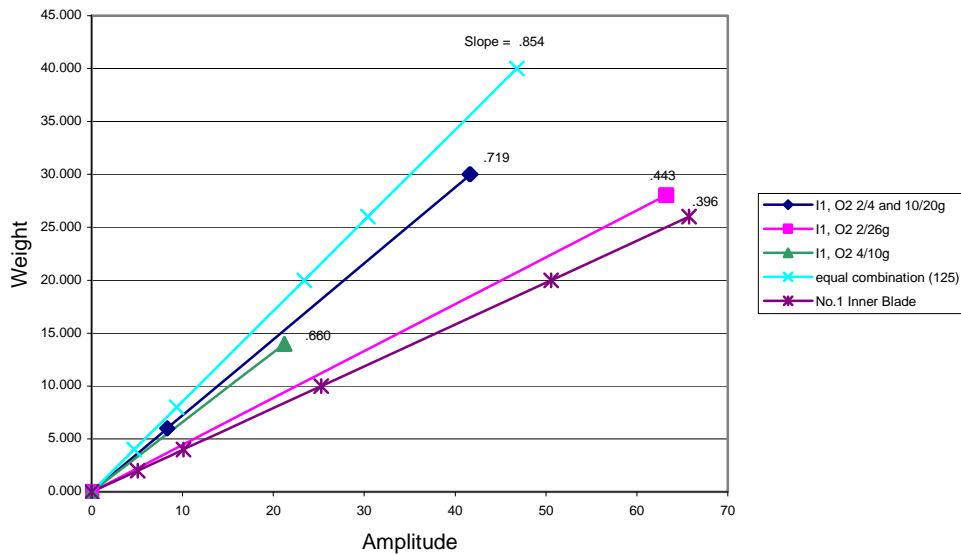


**Figure 33. 125 Degree Quadrant Weight to Amplitude Distribution**

It is evident that, in all three figures shown above, the slope increases as the weight becomes more equally distributed between the two blades bordering the specified

quadrant. There is enough evidence now to state that the maximum slope occurs when the weight is evenly distributed between the two bounding blades of a quadrant.

The final analysis compiles the slope data collected in the three different sized quadrants and determines its relationship to the phase. Each of the data points in Figure 34, Figure 35, and Figure 36 are the slope values from Figure 31, Figure 32, and Figure 33 respectively. In the following three figures, each quadrant displays a maximum value in the center of the quadrant and decreases to approximately 0.394-0.396 at the blade locations. The difference between 0.394 and 0.396 is one half of one percent and since the overall objective is to determine trends, it is recognized as insignificant. The symmetric qualities of the figures, and a well defined maximum, justify a second order polynomial to curve fit the charts. Due to the large phase values and smaller slope values, the algorithms established are more sensitive in the 55 and 90 degree quadrants. All the figures represent the fact that the algorithms displayed will provide values that are within a reasonable error (0.01 slope value distance) of the collected data.

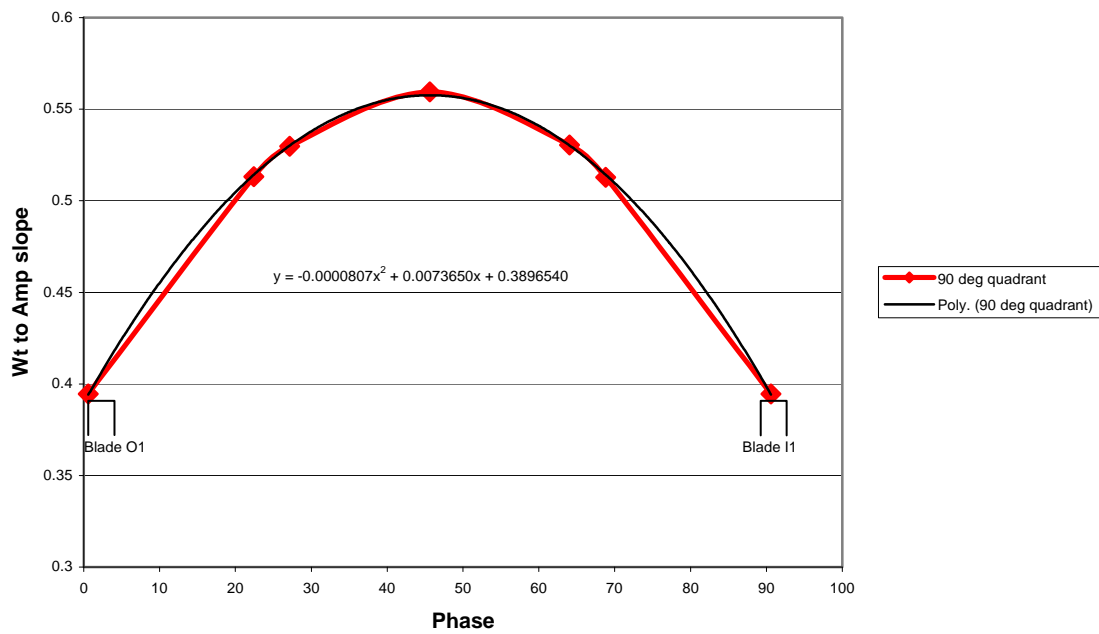


Figure 34. Slope Variation within a 90 Degree Quadrant

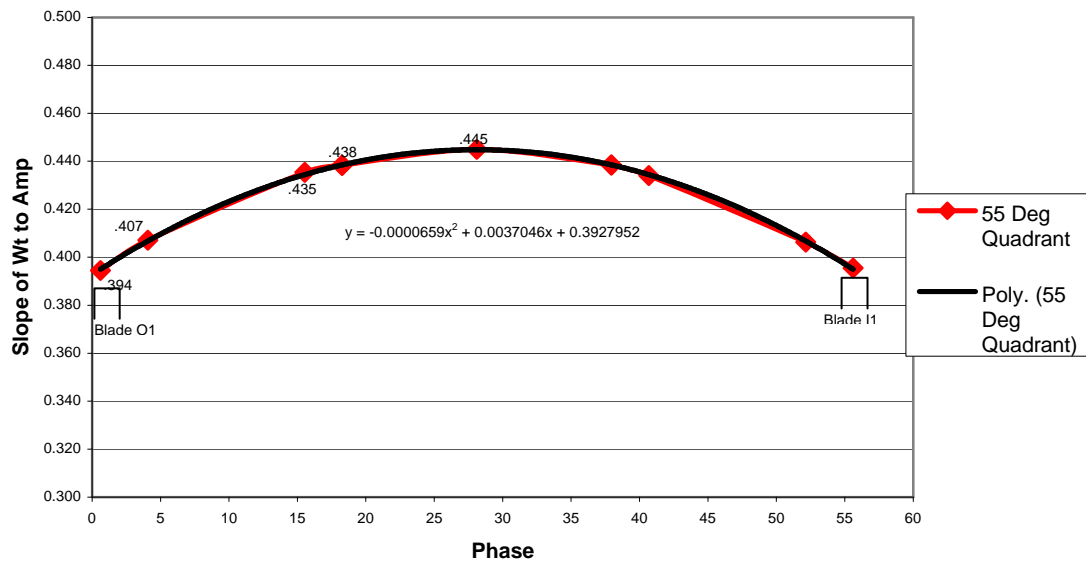
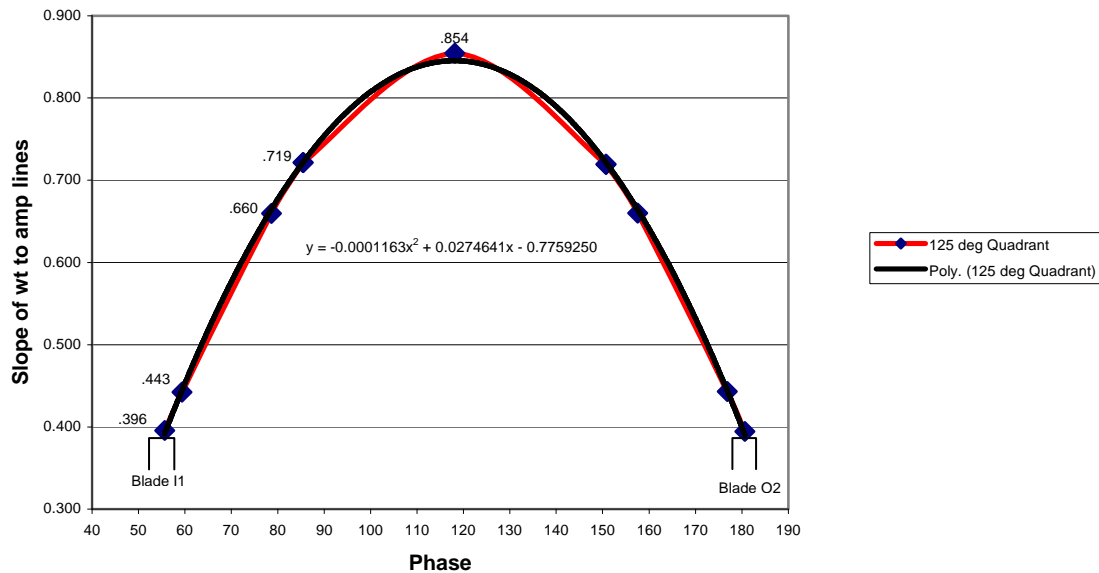
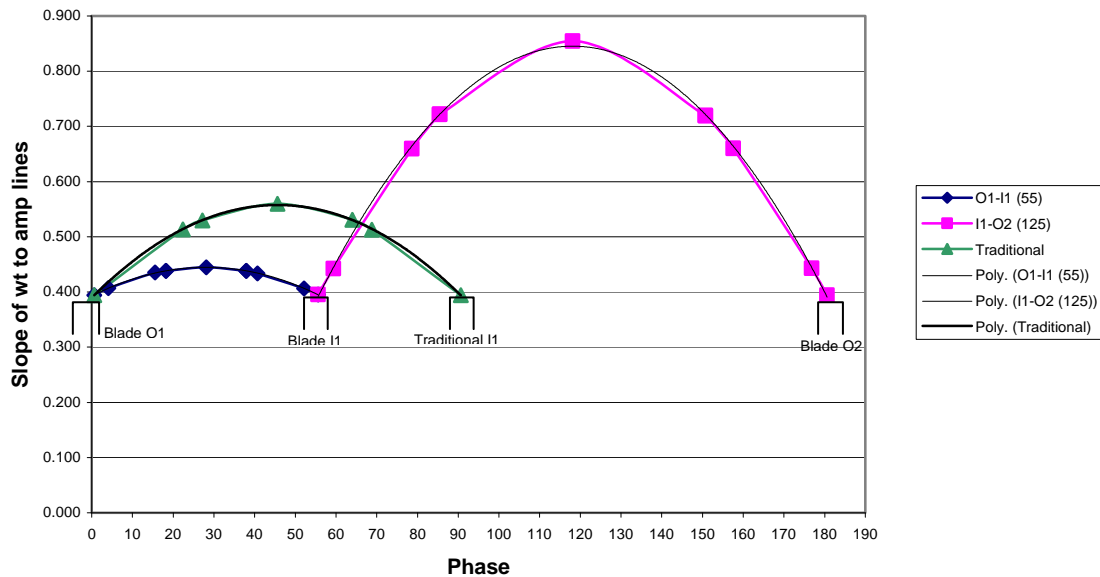


Figure 35. Slope Variation within a 55 Degree Quadrant



**Figure 36. Slope Variation within a 125 Degree Quadrant**

The 55 degree quadrant, Figure 35, contains the least amount of variation in the slope between the weight and amplitude, 0.051. The 90 degree quadrant, Figure 34, has a variation of 0.165 and the 125 degree quadrant, Figure 36, has a variation of 0.458. Figure 37 displays the results from Figure 35, Figure 34, and Figure 36 in a span of 180 degrees of phase. The blade locations are illustrated at their respective locations. The traditional blades, located at 0 and 90 degrees, are transposed into Figure 37. The variation of slope for the traditional blade is in yellow. The 55 and 125 degree quadrants are displayed in blue and magenta respectively.



**Figure 37. 0-180 Degree Phase Representation of Apache and Traditional Model**

It appears that the relationship between the variations increases drastically as the quadrant size approaches 180 degrees. In order to compare all three quadrants, the 125 degree quadrant was shifted to start at zero degrees of phase, the same point as the other quadrants. It is now apparent that the weight to amplitude slope has a non linear relationship to the quadrant size. Figure 38 shows that the quadrants maxima diverge as the quadrant size approaches 180 degrees. This is significant in the fact that, as the quadrant size differential increases (i.e. 55/125 differential is 70 degrees and a 35/145 differential is 110), the difference in weight correction factors, based on the quadrant, tend to exhibit a larger difference.

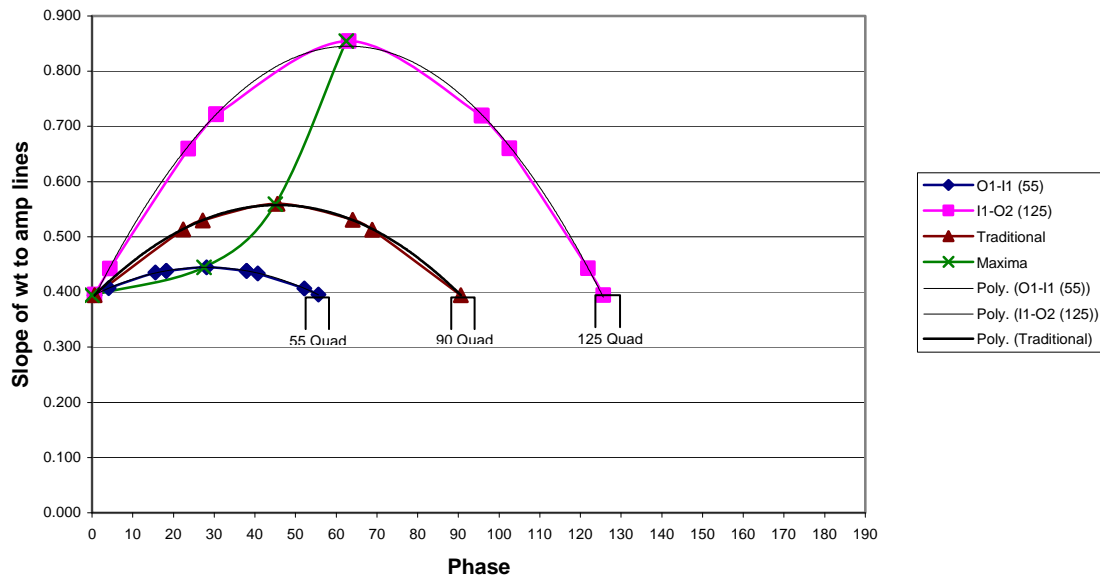


**Figure 38. 55, 90, and 125 Degree Quadrants Based at Zero Phase**

### Accelerometer in the Y (Lateral) Direction

In the problem statement, AMRDEC stated that one of the areas to research was to identify if it would be beneficial to add an accelerometer in the lateral direction. Most of the forces that are represented in the Y (lateral) direction are the aerodynamic forces generated by the blades. A chart depicting the Y forces with respect to the azimuth was generated for every simulation. Figure 39 represents the results found in every simulation; a small sinusoidal variation within the tolerances (0.5 lbf) set by the trim variable screen of the RCAS model. Based on the Apache RCAS tail rotor model, an accelerometer mounted in the Y direction will not measure a variation in accelerations dependent on a rotor system that is imbalanced or even balanced.

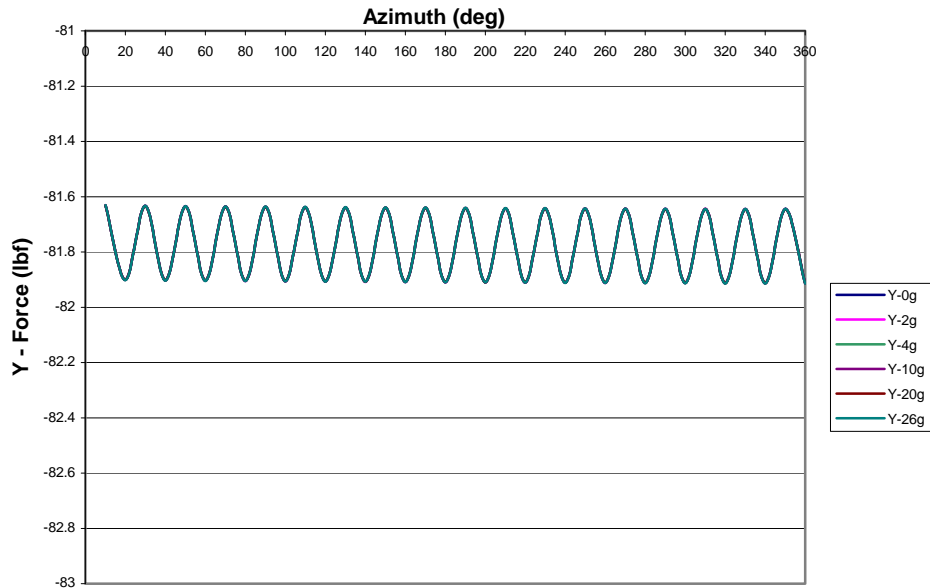


**Figure 39. Apache Model Y Force Distribution**

### **Accelerometer in the X (Longitudinal) Direction**

The capability also exists to develop a mount for an accelerometer to be mounted in the X direction. The Apache model created for RCAS is capable of analyzing the forces that exist in the X direction. This will allow the analysis of the forces prior to taking time and resources to design and manufacture a new mount. Figure 40 and Figure 27 are similar in that they both represent the amplitude and phase of the Apache model when 10 grams are added to adjacent blades. Their difference is in the direction of the forces. Figure 40 represents the forces in the X direction where the Y axis in Figure 26 is the force in the Z direction. The amplitudes in both figures appear to be the same however the phases are exactly 90 degrees apart. This observation continues to be true in every simulation.



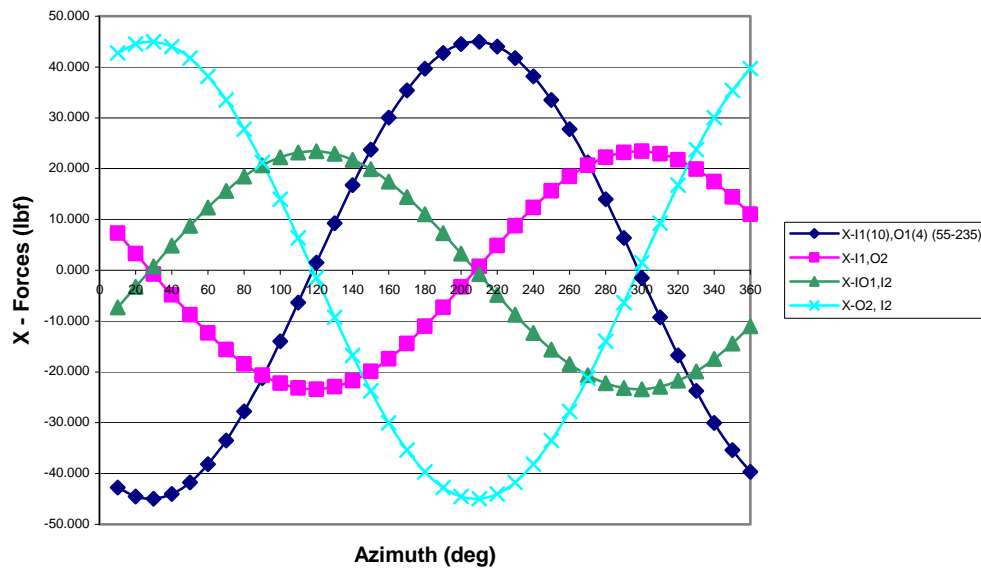


**Figure 40. X Force, Apache Model Equal wt (10)g to Adjacent Blades**

At first glance, the data displayed in the X direction does not appear to provide additional information, but it is possible that the resultant of the forces in the X and Z direction will lead to a simplified solution. Unfortunately, the resultant value of the X and Z forces produced a similar relationship between the phase and weight as the individual forces. In conclusion, there is no added value to collecting data from an accelerometer in the longitudinal direction with regards to its forces.

## Results and Analysis Conclusions

Although the data received by the operator is not displayed in amplitude forces, the data collected shows the balancing trends in forces depending on the quadrant size. Both the ips values displayed by the AVA computer and the Forces displayed by the RCAS model represent the magnitude of the imbalance, therefore the forces that are mathematically modeled by RCAS are used to show the aerodynamic trends of the

Apache tail rotor. With the evidence presented, the phase data provided in an imbalanced rotor system can be used to determine the slope of a weight to amplitude chart depending on the quadrant the phase is located in. Next, the amplitude information is used to determine the combined weight to be removed or added from the 2 blades bounding the quadrant. Equations 5 and 6 are simple formulas using the total weight and the phase to determine the weight required to add or remove from the specific blades. Blade “M” is the first blade with a lower phase number computed by the model. Blade “N” is the first blade with a higher phase number than the imbalanced phase computed. These blades represent the bounding blades that identify whether the quadrant size for the 55 degree quadrant. These equations do not work as well for the 125 degree quadrant, indicating that the phase angle can not be directly used to determine proportionality.

$$W_{Blade_M} = \frac{\Phi_{Blade_M} - \Phi_{calc.}}{Quadrant\_Size} \cdot (W_{Total}) \quad (5)$$

$$W_{Blade_N} = -\left(\frac{\Phi_{Blade_N} - \Phi_{calc.}}{Quadrant\_Size}\right) \cdot (W_{Total}) \quad (6)$$

The following is an example that can be used to show the process of determining an adjustment based on the phase angle and raw amplitude data collected by the AVA computer. A phase angle of 40.68 degrees is given and the amplitude is 32.25 lbf. The 40.38 degree phase angle places the imbalance between the inner No.1 and outer No.1 blades of the Apache model. The inner No.1 and outer No.1 blades bound a 55 degree quadrant. The phase angle is used in Figure 36 to determine the slope of the weight to amplitude line. In this example, the slope is 0.435. The next step uses Figure 33, the amplitude of 32.25, and the slope of 0.435 to determine the total weight needed to be

adjusted. The total weight is calculated to be 14 grams. Finally, apply the total weight and calculated phase to equations 5 and 6 to get an approximate weight distribution of -10.3g and -3.76g. This approximation is not as accurate with the 125 degree quadrants. The adjustments calculated with this method will be in the right direction; however the values will be off by approximately 15% to 30%. In order for more accurate results in the 125 degree quadrant more accurate methods need to be applied. This is a generic process that is feasible with the data computed by RCAS. A similar approach may be feasible with the phase and ips data computed by the AVA computer.

## **V: Conclusions**

### **Conclusions of Research**

The objective of this study was to develop a model of the Apache tail rotor with a comprehensive computer modeling analysis program and evaluate the tail rotor balancing procedures performed on the AH-64A/D Apache by the United States Army. A successful computer model was created using the RCAS computer modeling program. The goal of this study was to use the model to analyze the tail rotor system of the Apache and determine if the tail rotor balancing methods used by the Army could be improved. The current method used to balance the tail rotor identifies one sensitivity coefficient for the two inner blades and another sensitivity coefficient for the two outer blades. The research for this thesis indicates that the sensitivity coefficients are related to the different quadrant sizes, not the inner and outer blades.

The sensitivity coefficients used for AVA need to be reevaluated to focus on imbalances within different quadrants as opposed to a specific blade. Currently, the sensitivity coefficients applied to the adjustment algorithms are broken down into an outer blade coefficient and an inner blade coefficient. The evidence from the simulation results showed that the sensitivities depended on the quadrant the phase fell into, not the relationship between the inner and outer blades. That would mean every blade would have two sensitivity coefficients, one for the adjacent 55 degree quadrant and one for the adjacent 125 degree quadrant. The current sensitivity coefficients are based on multiple known adjustments and their corrections which ultimately end up being an average sensitivity between the two adjacent quadrants of that blade. The simulation results

showed that adjustments required if the phase fell in the 125 degree quadrant needed more total weight than if the phase fell into a 55 degree quadrant. Based on the Z force amplitudes, that weight difference could be twice as much in the 125 degree quadrant compared to the 55 degree quadrant.

Based on the results provided, no value is added by installing an accelerometer in the lateral (Y axis) or longitudinal (X axis) direction. Based on the data collected on the forces in the X and Y direction from the simulations, it does not appear to be beneficial to recreate an algorithm including these forces. The forces generated in the Y direction were primarily the aerodynamic forces generated by the rotor blades and are constant, not affected by imbalance. The forces in the X direction are essentially the same forces in the Z direction, with a 90 degree phase difference. There may be some added value in collecting the data to help identify indirect vibrations in the respective direction; however, it does not enhance the ability to balance the blades.

Tail rotor balancing, in general, can be a fairly quick process to complete during a maintenance test flight. When a maintenance test flight crew runs into problems balancing the tail rotor system, they have to shut down the helicopter, analyze the data, make the adjustments, have quality assurance approve the adjustments, restart the helicopter again, and rerun the analysis. If the tail rotor system isn't responding as expected, a considerable amount of time can be spent troubleshooting the problem. Every hour or day spent troubleshooting the tail rotor, is one less hour or day the Apache is not able to support the soldiers on the front line.

## **Suggestions for Future Research**

The RCAS model for the Apache tail rotor was designed to analyze different trends in an imbalanced Apache tail rotor. The Apache RCAS model was effective in identifying that the phase angle of an imbalanced rotor system has a direct relationship to the amplitude. Additionally, there was a distinct relationship between the phase angle and the amplitude based on the quadrant size. Finally, the RCAS results identified that less weight was required to produce the same amplitude in the 55 degree quadrant compared to the 125 degree quadrant; thus distinguishing the 55 degree quadrant as being more sensitive to weight adjustments. While this thesis was effective in identifying the phase angle, amplitude, and weight relationships, the model could be modified to produce more accurate numbers which could lead to actually calculating the sensitivity coefficients needed for the AVA computer. Future methods integrated with the AVA computer can be developed in order to better define the actual sensitivity coefficients used to proportionate the total weight and use that coefficient for real world applications.

The AVA computer currently contains two sensitivity coefficients, one for the inner blades, and one for the outer blades. Each blade has an adjacent 55 degree quadrant and a 125 degree quadrant. The current adjustment methods allow for the same sensitivity coefficient to be applied to either sized quadrant. The information collected from the Apache tail rotor RCAS model should provide enough validation for the Army to investigate new sensitivity coefficients based on the 55 degree and 125 degree quadrants to replace the current sensitivity coefficients for the inner and outer blades to improve the tail rotor balancing procedures for the AH-64A/D Apache.

## Bibliography

1. Taitel, H., Danai, K., Gauthier, D., "Helicopter Track and Balance With Artificial Neural Nets," *AMSE Journal of Dynamic Systems, Measurement, and Control*, Vol. 117 No. 2, June 1995, pp 226-231
2. Renzi, Michael J. *An Assessment of Modern Methods for Rotor Track and Balance*. MS Thesis, AFIT/GAE/ENY/04-J11. Graduate School of Engineering and Management Air Force Institute of Technology, Wright Patterson AFB OH, June 2004
3. Miller, Nathan A. *A Comparison of Main Rotor Smoothing Adjustments Using Linear and Neural Network Algorithms*. MS Thesis, AFIT/GAE/ENY/06-M24. Graduate School of Engineering and Management Air Force Institute of Technology, Wright Patterson AFB OH, June 2006.
4. Pritchard, James A. *A Redesigned Tail Rotor for Improvement of CH-53E High Altitude Performance*. MS Thesis, AFIT/GAE/ENY/05-M27. Graduate School of Engineering and Management Air Force Institute of Technology, Wright Patterson AFB OH, June 2005.
5. Leishman, J.G., Principles of Helicopter Aerodynamics, Press Syndicate of the University of Cambridge, United Kingdom, 2006.
6. USAAMCOM/AFDD, "RCAS Users Manual, Rotorcraft Comprehensive Analysis System, Version 2.0," TR 02-A-006, Moffett Field, CA, May 2003.
7. Department of the Army, "Operators Manual for Helicopter, Attack, AH-64A Apache," TM 1-1520-238-10 C11, United States Army, Chief of Staff, Pentagon, 2003.
8. Winn, A. *Longbow Apache Air Vehicle Technical Description*. McDonnell Douglas Helicopter Company, Mesa, AZ, 1991.
9. Dendy, J.C., Landers C.L. *YAH-64 Advanced Attack Helicopter Design*. American Helicopter Society, Annual National Forum, 31<sup>st</sup>, Washington, D.C., May 1975.
10. Prouty R.W., Amer K.B. *The YAH-64 Empanage and Tail Rotor – A Technical History*. American Helicopter Society, Annual National Forum, 38<sup>th</sup>, Washington, D.C., May 1982.
11. Kunz, Donald L. Class Notes, AERO 610, Rotorcraft Aeromechanics. School of Engineering and Management Air Force Institute of Technology, Wright Patterson AFB OH, Fall 2006.
12. Keller, Jonathan A. Engineer, Aviation and Missile Research Development and Engineering Center (AMRDEC), Huntsville, AL. Correspondence. 2006-2007.
13. Raymer, Daniel P. *Aircraft Design: A Conceptual Approach*, American Institute of Aeronautics, Inc., Reston, VA, 1999.
14. Jones, Henry E., Kunz, Donald, L., *Comprehensive Modeling of the Apache in CAMRAD II*. American Helicopter Society, Hampton Roads Chapter, Structural Specialists Meeting, Williamsburg, VA, November 2001.

15. Irvine, Tom. "Shock and Vibration Response Spectra and Software."  
[http://www.vibrationdata.com/Newsletters/April2003\\_NL.pdf](http://www.vibrationdata.com/Newsletters/April2003_NL.pdf). April 2003.
16. Jackson, Paul. *Jane's All the World's Aircraft*. Great Britain: Cambridge University Press, 2001-2002, 2006-2007.
17. Department of the Army. *Technical Manual for Test Set Aviation Vibration Analyzer (AVA)*. TM 1-6625-724-13&P. Headquarters, Department of the Army, Pentagon Washington DC, March 2002.



## Appendix A: AH-64 Apache Tail Rotor RCAS Input File

```

MENU RCASROOT
11
E
1
COMMAND
!=====
!===== STRUCTURAL MODEL =====
!=====
s GFRAMEORIG
!
! IDENTIFY G FRAME NODE AND ACTIVE DOFS
!
! Primitive Active Degrees of Freedom
! Subsystem Structure Node Translational Rotational
! Name Name ID X Y Z X Y Z
a FUSE TRFUSE 10 1 0 1 0 0 1
! *****
n
!
! DEFINE PROPERTIES FOR TRIM SPRINGS AND DAMPERS
! Type ----- Translational ----- ----- Rotational -----
! SPR/DMP KX1 KX2 KX3 KThetax KThetay KThetaz
a DMP 3.240e+04 3.240e+04 3.240e+04 1.360e+06 4.960e+07 5.660e+07
a SPR 2.200e+05 2.200e+05 2.200e+05 1.500e+07 3.500e+08 4.000e+08
! *****
s SUBSYSIDS
!
! LIST THE SUBSYSTEMS WHICH COMPRISE THE MODEL
! Subsystem Name(s)
a FUSE
a TROTORI
a TROTORO
! *****
s SSORIGIN
!
! DEFINE SUBSYSTEM LOCATION WITH RESPECT TO GLOBAL (G) FRAME
! Subsystem Origin Coordinates
! Name x y z
a FUSE 0. 0. 0.
a TROTORI -1. -2.4683 0.
a TROTORO -1. -2.96 0.
! *****
s SSORIENT
!
! DEFINE SUBSYSTEM ORIENTATION WITH RESPECT TO GLOBAL (G) FRAME
! Subsystem rotation 1 rotation 2 rotation 3
! Name axis angle(deg) axis angle(deg) axis angle(deg)
a FUSE 2 0. 1 0. 0 0.
a TROTORI 2 180. 1 -90. 0 0.
a TROTORO 2 180. 1 -90. 0 0.
! *****
s CONTROLMIXER
!
! DEFINE LINEAR RELATION BETWEEN PILOT INPUT AND CONTROL SURFACES
! Control Value at zero ----- Coefficients for Pilot Control -----
! ID pilot control Coll. Lat. Long. Pedal Throt
a 1 0. 0. 0. 0. 1.7453E-02 0.
! *****
s ROTNONCONST
!
! DEFINE ROTATING-TO-NONROTATING INTERFACE(S)
! ----- Node 1 ----- ----- Node 2 -----
! Cnstr. Subsystem Primitive Node Subsystem Primitive Node
! ID Name Name ID Name Name ID
!
a 1 FUSE TRFUSE 50 TROTORI TRHUBI 50

```

```

a   2          FUSE          TRFUSE          60          TROTORO          TRHUBO          60
! *****
!=====
!===== BEGIN SUBSYSTEM =====
!
!                               FUSE
s SELSUBSYS
! Subsystem Name
a   FUSE
s SUBSYSTYP
!   Subsystem Type
!   1. Rotor (rotating), 2. Fuselage (nonrotating), 3. Control system
a   2
s SUBSYSCOMP
!
!   LIST THE PRIMITIVE STRUCTURES WHICH COMPRISE THE SUBSYSTEM
!
!   Primitive Structure
!
!   Name
a   TRFUSE
! *****
s PSORIGIN
!
!   Primitive          Primitive Origin Offset
!   Name              x      y      z
!
!
a   TRFUSE              0.    0.    0.
! *****
s PSORIENT
!
!   PRIMITIVE STRUCTURE ORIENTATION WITH RESPECT TO THE SUBSYSTEM
!
!   Primitive      rotation 1      rotation 2      rotation 3
!   Name          axis angle(deg)  axis angle(deg)  axis angle(deg)
a   TRFUSE        2      0.        1      0.        0      0.
! *****
!===== BEGIN PRIMITIVE STRUCTURE =====
!
!                               TRFUSE
s PRIMITIVEID
!
!   IDENTIFY PRIMITIVE STRUCTURE(S) TO BE EDITED OR CREATED
!
!   Primitive Structure Name(s)
a   TRFUSE
! *****
s ELDATASETID
!
!   IDENTIFY THE ELEMENT DATA TABLE FOR THE PRIMITIVE
!
!   Element Data Table Name
a   ELPROP
! *****
s FENODE
!
!   DEFINE STRUCTURAL NODES DIRECTLY
!
!   Node          Node Coordinates (feet)
!   ID            x      y      z
a   10            0.    0.    0.
a   50            -1. -2.4683  0.
a   60            -1. -2.96   0.
! *****
s RBMELE
!
!   DEFINE RIGID BODY MASS ELEMENT(S)
!
!   Element      Node      Property
!   ID           ID        ID
a   2           10         1
! *****
s RIGIDBAR
!
!   DEFINE RIGID BAR ELEMENT(S)
!
!   Element      Node1 Node2      Center of gravity offset
!   ID           ID    ID          X      Y      Z
a   4           10    50          0.    0.    0.

```

```

a      5      10      60      0.      0.      0.
!
!===== TRFUSE =====
!===== END PRIMITIVE STRUCTURE =====
!
!===== FUSE =====
!===== END SUBSYSTEM =====
!=====
!===== BEGIN SUBSYSTEM =====
!
!
!===== TROTORI =====

s SELSUBSYS
!   Subsystem Name
a      TROTORI
! *****
s SUBSYSTYP
!   DESIGNATE THE SUBSYSTEM TYPE
!   1. Rotor (rotating), 2. Fuselage (nonrotating), 3. Control system
a      1
! *****
s SUBSYSCOMP
!   LIST THE PRIMITIVE STRUCTURES WHICH COMPRISE THE SUBSYSTEM
!   Primitive Structure
!   Name
a      TRHUBI
a      TBLADEI1
a      TBLADEI2
! *****
s CORNODE
!   DEFINE CENTER OF ROTATION NODE FOR A ROTOR
!   Primitive      Rotor/Shaft      Torque      Rotor Reference
!   Structure      Connection      Bearing      Azimuth ID
!   Name           Node ID          Defined      SSname_PSname_ELname
a      TRHUBI      50              0
! *****
s BLADECOMP
!
!   DEFINE BLADE COMPOSITION
!   Blade          Primitive Structure Name(s)
!   Index      1      2      3      4      5      6      7
a      1  TBLADEI1  --      --      --      --      --      --
a      2  TBLADEI2  --      --      --      --      --      --
! *****
s PSORIGIN
!   PRIMITIVE STRUCTURE LOCATION WITH RESPECT TO SUBSYSTEM
!   Primitive          Primitive Origin Offset
!   Name              x      y      z
a      TRHUBI          0.0    0.0    0.0
a      TBLADEI1         0.     0.     0.
a      TBLADEI2         0.     0.     0.
! *****
s PSORIENT
!   PRIMITIVE STRUCTURE ORIENTATION WITH RESPECT TO THE SUBSYSTEM
!   Primitive          rotation 1      rotation 2      rotation 3
!   Name              axis angle(deg)  axis angle(deg)  axis angle(deg)
a      TRHUBI          3 0.0            2 0.0            1 0.0
a      TBLADEI1         3 -55.0          2 0.0            1 0.0
a      TBLADEI2         3 -235.0         2 0.0            1 0.0
! *****
s CONNCONST
!
!   CONNECTIVITIES BETWEEN PRIMITIVE STRUCTURES

```

```

!      Constr.      Primitive      Node  Primitive      Node
!      ID           Name of Child  ID    Name of Parent  ID
a      1            TBLADEI1       50    TRHUBI         51
a      2            TBLADEI2       50    TRHUBI         51
! *****
s ROTORPARAM
!
!              INPUT ROTOR SPEED
!      Rotor Rotational
!      Speed (rad/sec)
!
a      148.4302
! ***
! *****
!===== BEGIN PRIMITIVE STRUCTURE =====
!
!              TRHUBI
!
s PRIMITIVEID
!
!      IDENTIFY PRIMITIVE STRUCTURE(S) TO BE EDITED OR CREATED
!      Primitive Structure Name(s)
a      TRHUBI
! *****
s ELDATASETID
!
!      IDENTIFY THE ELEMENT DATA TABLE FOR THE PRIMITIVE
!      Element Data Table Name
a      ELPROP
! *****
s FENODE
!
!      DEFINE STRUCTURAL NODES DIRECTLY
!      Node      Node Coordinates (feet)
!      ID        x      y      z
a      50        0.      0.      0.
a      51        0.      0.      0.
! *****
s RBMELE
!
!      DEFINE RIGID BODY MASS ELEMENT(S)
!      Element    Node      Property
!      ID         ID       ID
a      1         50        1
a      2         51        1
! *****
s HINGE
!
!      DEFINE HINGE ELEMENTS
!      Element    Node1  Node2  Hinge Free or      Spring      Damper
!      ID         ID    ID    Type Controlled  Constant    Constant
a      3         50    51    YHIN      0          0.0        0.0
n
!
!      DEFINE HINGE ELEMENT(S) DIRECTION
!      Element    Hinge Angles (deg) wrt Primitive Structure
!      ID         x      y      z
A      3         0.0    0.0    0.0
! *****
!
!              TRHUBI
!===== END PRIMITIVE STRUCTURE =====
!===== BEGIN PRIMITIVE STRUCTURE =====
!
!              TBLADEI1
s PRIMITIVEID
!
!      IDENTIFY PRIMITIVE STRUCTURE(S) TO BE EDITED OR CREATED
!      Primitive Structure Name(s)
a      TBLADEI1
! *****

```

```

s ELDATASETID
!
! IDENTIFY THE ELEMENT DATA TABLE FOR THE PRIMITIVE
! Element Data Table Name
a ELPROP
! *****
s FENODE
!
! DEFINE STRUCTURAL NODES DIRECTLY
! Node Node Coordinates (feet)
! ID x y z
a 50 0. 0. 0.
a 70 4.58 0. 0.
! *****
s RIGIDBLADE
!
! DEFINE RIGID BLADE ELEMENT
! Element Node Prop Hinge Sequence number (0-3)
! ID ID ID Lead-Lag Flap Pitch Bearing
a 1 50 2 0 0 0
! *****
s CONTROLCONNECT
!
! DEFINE CONTROL CONNECTION TO ELEMENTS
! Control Swashplate Swashplate Element Type Element
! ID or Direct Phase(deg) (HIN/AUX/MLD ...) or ACP ID
a 1 SPCOLL 0.0 RBE 1
!
! TBLADEI1
!===== END PRIMITIVE STRUCTURE =====
!===== BEGIN PRIMITIVE STRUCTURE =====
!
! TBLADEI2
s PRIMITIVEID
!
! IDENTIFY PRIMITIVE STRUCTURE(S) TO BE EDITED OR CREATED
! Primitive Structure Name(s)
a TBLADEI2
! *****
s ELDATASETID
!
! IDENTIFY THE ELEMENT DATA TABLE FOR THE PRIMITIVE
! Element Data Table Name
a ELPROP
! *****
s FENODE
!
! DEFINE STRUCTURAL NODES DIRECTLY
! Node Node Coordinates (feet)
! ID x y z
a 50 0. 0. 0.
a 70 4.58 0. 0.
! *****
s RIGIDBLADE
!
! DEFINE RIGID BLADE ELEMENT
! Element Node Prop Hinge Sequence number (0-3)
! ID ID ID Lead-Lag Flap Pitch Bearing
a 1 50 2 0 0 0
! *****
s CONTROLCONNECT
!
! DEFINE CONTROL CONNECTION TO ELEMENTS
! Control Swashplate Swashplate Element Type Element
! ID or Direct Phase(deg) (HIN/AUX/MLD ...) or ACP ID
a 1 SPCOLL 0.0 RBE 1
!
!S PRIMIT
!A 1 TBLADEI1 TBLADEI2
!
! TBLADEI2
!===== END PRIMITIVE STRUCTURE =====
!
! TROTORI

```

```

!===== END SUBSYSTEM =====
!=====
!===== BEGIN SUBSYSTEM =====
!
!                               TROTORO
s SELSUBSYS
!   Subsystem Name
a   TROTORO
! *****
s SUBSYSTYP
!   DESIGNATE THE SUBSYSTEM TYPE
!   1. Rotor (rotating), 2. Fuselage (nonrotating), 3. Control system
a   1
! *****
s SUBSYSCOMP
!   Primitive Structure
!   Name
a   TRHUBO
a   TBLADE01
a   TBLADE02
! *****
s CORNODE
!   DEFINE CENTER OF ROTATION NODE FOR A ROTOR
!   Primitive      Rotor/Shaft Torque      Rotor Reference
!   Structure      Connection
!   Bearing        Azimuth ID
!   Name           Node ID      Defined      SSname_PSname_ELname
a   TRHUBO         60    0
! *****
s BLADECOMP
!   DEFINE BLADE COMPOSITION
!   Blade           Primitive Structure Name(s)
!   Index           1      2      3      4      5      6      7
!
a   1               TBLADE01 --      --      --      --      --      --
a   2               TBLADE02 --      --      --      --      --      --
! *****
s PSORIGIN
!   PRIMITIVE STRUCTURE LOCATION WITH RESPECT TO SUBSYSTEM
!   Primitive      Primitive Origin Offset
!   Name           x           y           z
a   TRHUBO         0.0        0.0        0.0
a   TBLADE01       0.0        0.0        0.0
a   TBLADE02       0.0        0.0        0.0
! *****
s PSORIENT
!   PRIMITIVE STRUCTURE ORIENTATION WITH RESPECT TO THE SUBSYSTEM
!   Primitive      rotation 1      rotation 2      rotation 3
!   Name           axis angle(deg) axis angle(deg) axis angle(deg)
a   TRHUBO         3      0.0      2      0.0      1      0.0
a   TBLADE01       3      0.0      2      0.0      1      0.0
a   TBLADE02       3     -180.0     2      0.0      1      0.0
! *****
s CONNCONST
!   CONNECTIVITIES BETWEEN PRIMITIVE STRUCTURES
!   Constr.      Primitive      Node      Primitive      Node
!   ID           Name of Child ID      Name of Parent ID
a   1            TBLADE01       60      TRHUBO         61
a   2            TBLADE02       60      TRHUBO         61
! *****
s ROTORPARAM

```

```

!           INPUT ROTOR SPEED
!           Rotor Rotational
!
a           148.4302
!===== BEGIN PRIMITIVE STRUCTURE =====
!
!           TRHUBO
s PRIMITIVEID
!           IDENTIFY PRIMITIVE STRUCTURE(S) TO BE EDITED OR CREATED
!           Primitive Structure Name(s)
a           TRHUBO
! *****
s ELDATASETID
!           IDENTIFY THE ELEMENT DATA TABLE FOR THE PRIMITIVE
!           Element Data Table Name
a           ELPROP
! *****
s FENODE
!           DEFINE STRUCTURAL NODES DIRECTLY
!           Node           Node Coordinates (feet)
!           ID            x            y            z
a           60            0.            0.            0.
a           61            0.            0.            0.
! *****
s RBMELE
!           DEFINE RIGID BODY MASS ELEMENT(S)
!           Element       Node   Property
!           ID            ID     ID
a           1            60      1
a           2            61      1
! *****
s HINGE
!           DEFINE HINGE ELEMENTS
!           Element       Node1 Node2 Hinge       Free or   Spring   Damper
!           ID            ID     ID   Type        Controlled Constant Constant
a           3            60      61   YHIN         0         0.0     0.0
n
! DEFINE HINGE ELEMENT(S) DIRECTION
!           Element       Hinge Angles (deg) wrt Primitive Structure
!           ID            x            y            z
a           3            0.0         0.0         0.0
! *****
!
!           TRHUBO
!===== END PRIMITIVE STRUCTURE =====
!===== BEGIN PRIMITIVE STRUCTURE =====
!
!           TBLADE01
s PRIMITIVEID
!           IDENTIFY PRIMITIVE STRUCTURE(S) TO BE EDITED OR CREATED
!           Primitive Structure Name(s)
a           TBLADE01
! *****
s ELDATASETID
!           IDENTIFY THE ELEMENT DATA TABLE FOR THE PRIMITIVE
!           Element Data Table Name
a           ELPROP
! *****
s FENODE
!           DEFINE STRUCTURAL NODES DIRECTLY
!           Node           Node Coordinates (feet)
!           ID            x            y            z
a           60            0.            0.            0.
a           70            4.58         0.            0.

```

```

! *****
s RIGIDBLADE
!
!       DEFINE RIGID BLADE ELEMENT
!       Element      Node      Prop      Hinge Sequence number (0-3)
!       ID           ID       ID       Lead-Lag      Flap      Pitch Bearing
a       1           60       3         0             0             0
! *****
s CONTROLCONNECT
!
!       DEFINE CONTROL CONNECTION TO ELEMENTS
!       Control      Swashplate      Swashplate      Element Type      Element
!       ID           or Direct      Phase(deg) (HIN/AUX/MLD ...) or ACP ID
a       1           SPCOLL          0.0             RBE             1
!
!                               TBLADE01
!===== END PRIMITIVE STRUCTURE =====
!===== BEGIN PRIMITIVE STRUCTURE =====
!
!                               TBLADE02
s PRIMITIVEID
!
!       IDENTIFY PRIMITIVE STRUCTURE(S) TO BE EDITED OR CREATED
!       Primitive Structure Name(s)
a       TBLADE02
! *****
s ELDATASETID
!
!       IDENTIFY THE ELEMENT DATA TABLE FOR THE PRIMITIVE
!       Element Data Table Name
A       ELPROP
! *****
s FENODE
!
!       DEFINE STRUCTURAL NODES DIRECTLY
!       Node              Node Coordinates (feet)
!       ID              x      y      z
a       60              0.     0.     0.
a       70              4.58   0.     0.
! *****
s RIGIDBLADE
!
!       DEFINE RIGID BLADE ELEMENT
!       Element      Node      Prop      Hinge Sequence number (0-3)
!       ID           ID       ID       Lead-Lag      Flap      Pitch Bearing
a       1           60       2         0             0             0
! *****
s CONTROLCONNECT
!
!       DEFINE CONTROL CONNECTION TO ELEMENTS
!       Control      Swashplate      Swashplate      Element Type      Element
!       ID           or Direct      Phase(deg) (HIN/AUX/MLD ...) or ACP ID
A       1           SPCOLL          0.0             RBE             1
!S PRIMIT
!A 3 TBLADE01 TBLADE02
!
!                               TBLADE02
!===== END PRIMITIVE STRUCTURE =====
!
!                               TROTORI
!===== END SUBSYSTEM =====
!=====
! Copy primitive structures
EXIT
COMMAND
!COPYPRIMSTRUCT
!COMMAND
!=====
!===== BEGIN STRUCTURAL PROPERTIES =====
!===== ELEMENT PROPERTIES =====
s ELEPROPID
!
!       IDENTIFY THE ELEMENT DATA TABLE TO BE EDITED OR CREATED

```



```

a ELPROP
! *****
s RBMPRP
! INPUT RIGID BODY MASS ELEMENT PROPERTIES
!      Prop      Mass      ----- C.G. Offset (ft) -- Inertia Tensor (slug-ft**2)
!      ID      (slug)      x_1^E   x_2^E   x_3^E      |Ixx Ixy Ixz|
!                                          |Iyy Iyz Izz|
a      1      1.E-05      0.      0.      0.      0. 0. 0. 0. 0. 0.
! *****
s RBEPRP
! SPECIFY RIGID BLADE LEAD LAG HINGE PROPERTIES
! ----- Lead-lag Hinge -----
!      Prop_id      Hinge_Offset      Mass      Damping      Stiffness
!      (ft)      (slugs)      (lbs-sec/rad) (ft-lbs/rad)
a      2      0.      0.      0.      0.
a      3      0.      0.      0.      0.
! *****
n
! SPECIFY RIGID BLADE FLAP HINGE PROPERTIES
! ----- Flap Hinge -----
!      Prop_id      Hinge_Offset      Mass      Damping      Stiffness
!      (ft)      (slugs)      (lbs-sec/rad) (ft-lbs/rad)
a      2      0.      0.      0.      0.
a      3      0.      0.      0.      0.
! *****
n
! SPECIFY RIGID BLADE PITCH BEARING PROPERTIES
! ----- Pitch Bearing -----
!      Prop_id      Hinge_Offset      Mass      Damping      Stiffness
!      (ft)      (slugs)      (lbs-sec/rad) (ft-lbs/rad)
a      2      0.      0.      0.      0.
a      3      0.      0.      0.      0.
! *****
n
! SPECIFY RIGID BLADE PROPERTY DATA
! CURRENT_ELEMENT_PROPERTY_DATA_SET_ID: ELPROP
!      Prop_id      Blade_Mass      Blade-CG      Ixx      Iyy
!      (slugs)      (ft)      (slug-ft**2) (slug-ft**2)
a      2      .58      1.6787      .01767      1.009
a      3      .580685219      1.6787      .01767      1.009
! *****
!
!===== END STRUCTURAL PROPERTIES =====
!=====
!
!=====
!===== AERODYNAMIC MODEL =====
!=====
!
s AEROMODCOMP
! LIST THE NAMES OF THE AERODYNAMIC SUPERCOMPONENTS FOR THE MODEL
! Supercomponent Name
a ATROTORI
a ATROTORO
! *****
s SCORIGIN
! SUPERCOMPONENT POSITION WITH RESPECT TO GLOBAL FRAME
! Supercomponent Origin Coordinates
! Name      x      y      z
a ATROTORI      -1.0      -2.4683      0.0

```

```

a      ATROTORO      -1.0      -2.96      0.0
! *****
s SCORIENT
!      SUPERCOMPONENT ORIENTATION WITH RESPECT TO GLOBAL (G) FRAME
!      Supercomponent rotation 1 rotation 2 rotation 3
!      Name      axis angle(deg)      axis angle(deg)      axis angle(deg)
a      ATROTORI      2      180.      1      -90.      2      0.
a      ATROTORO      2      180.      1      -90.      2      0.
! *****
s AIRFOIL
!      IDENTIFY 2-D AIRFOIL TABLES (Table Look-Up)
!      Airfoil      Quasi Steady Airloads
!      ID      2D Table File Name
a      TBLADEAF      naca63414m_analytic.c81
! *****
s INTERFERENCE
!      AERODYNAMIC INTERFERENCE FOR SUPERCOMPONENTS
!      Row      Supercomponent Names      Interference      Interference
!      ID      From      TO      Model      Velocity Limit
a      1      ATROTORI      ATROTORO      SIMPLE-ROTOR-TO-ROTOR      0.0
*****
!=====
!===== BEGIN AERODYNAMIC SUPERCOMPONENT =====
! ATROTORI
s AEROSUPCOMPID
!      IDENTIFY THE SUPERCOMPONENT TO BE EDITED OR CREATED
a ATROTORI
! *****
s SUPCMPTYP
!      DESIGNATE THE SUPERCOMPONENT TYPE
! 1. Rotor
! 2. Wing
! 3. Body
! 4. Aux. Rotor
! 5. Bailey Rotor
! 6. Ducted Fan
a      1
! *****
s COMPID
!      LIST THE AERO COMPONENTS WHICH COMPRISE THE CURRENT SUPERCOMPONENT
!      Aerodynamics Primitive      Auxrotor/      Wing Left      End Wing
!      Component      Structure      Body/Wing      or Blade TIP      Right End
!      Name(s)      Name(s)      Root EL_ID      Node_ID      Node_ID
a      ATBLDEI1      TBLADEI1      0      70      0
a      ATBLDEI2      TBLADEI2      0      70      0
! *****
s CPORIGIN
!      COMPONENT LOCATION WITH RESPECT TO THE SUPERCOMPONENT
!      Component      Component Origin Offset
!      Name      x      y      z
a      ATBLDEI1      0.      0.      0.
a      ATBLDEI2      0.      0.      0.
! *****
s CPORIENT
!      COMPONENT ORIENTATION WITH RESPECT TO THE SUPERCOMPONENT
!      Component      rotation 1      rotation 2      rotation 3
!      Name      axis angle(deg)      axis angle(deg)      axis angle(deg)
a      ATBLDEI1      3      -55.      2      0.      1      0.
a      ATBLDEI2      3 -235.      2      0.      1      0.
! *****
s SUPCMPTOSS

```

```

!          STRUCTURAL SUBSYSTEM ASSOCIATED WITH THE CURRENT SUPERCOMPONENT
!          Subsystem Name
a          TROTORI
! *****
s INFLOW
!          SELECT INFLOW MODEL
! Inflow Model
! 0. No inflow
! 1. Uniform momentum inflow (half wings and rotors)
! 2. Uniform momentum inflow (full wings)
! 3 Peters and He inflow model (rotors only)
! 4. Wing free wake (Not supported yet)
! 5. Prescribed vortex wake (rotors only)
! 6. Free vortex wake (Scully)
! 7. Wind turbine induction flow (rotors only)
a          1
! *****
s AEROPTION
!          SELECT HIGHER ORDER AERODYNAMIC MODELING OPTIONS
!          Yawed      Tip      Linear      Nonlinear      Linear      Compress
!          Flow      Loss      Unsteady   Unsteady/Dyn      Stall Airfoil  -ibility
!          Effects   Option   Effects   Leishman-beddos/Onera Coeffs      Effects
!          (0:1)     (0:1)     (0:1)     (0:6)             (0:1)         (0:1)
a          1         1         1         0                 0             0
! *****
s TIPLOSS
!          INPUT DATA FOR SIMPLE TIP LOSS
!          Radial Location
!          for Zero Lift
!          (nondim)
a          0.95
! *****
s THRUSTAVE
!          INPUT DATA FOR THRUST AND TIP PATH PLANE ANGLE AVERAGING
!          Thrust Average #      Time Steps      Prescribed      # of Revolutions
!          Option                In Thrust Ave.      Thrust          to Average TPP
a          2                     36                .000001         1
!===== BEGIN AERODYNAMIC COMPONENT =====
!                                     ATBLDEI1
s AEROCOMPID
! Component name to be defined or modified
a ATBLDEI1
! *****
s COMPTYPE
!          DESIGNATE THE COMPONENT TYPE
! 1. Lifting Surface
! 2. BodyInternal.Loads
! 3. Aux/tail rotor
a          1
! *****
s AERONODE
!          DEFINE AERODYNAMIC NODE POINTS DIRECTLY
!          Node      ----- Coordinates -----
!          ID        1          2          3
a          21        1.05        0.0        0.0
a          22        1.283       0.0        0.0
a          23        1.808       0.0        0.0
a          24        2.083       0.0        0.0
a          25        2.5         0.0        0.0
a          26        2.917       0.0        0.0
a          27        3.333       0.0        0.0

```

```

a      28      3.75      0.0      0.0
a      29      4.167     0.0      0.0
a      30      4.58      0.0      0.0
! *****
s AEROSEG
!      DEFINE AERODYNAMIC SEGMENTS DIRECTLY
!      Seg.   Aerodyn   Node IDs   Chord   Airfoil   Element   Twist
!      ID     (Inboard) (Outboard) (ft)     ID         ID         (rad)
a      21      21       22       0.303 TBLADEAF  0         0.209
a      22      22       23       0.561 TBLADEAF  0         0.1903
a      23      23       24       0.833 TBLADEAF  0         0.1805
a      24      24       25       0.833 TBLADEAF  0         0.1655
a      25      25       26       0.833 TBLADEAF  0         0.1506
a      26      26       27       0.833 TBLADEAF  0         0.1356
a      27      27       28       0.833 TBLADEAF  0         0.1207
a      28      28       29       0.833 TBLADEAF  0         0.1057
a      29      29       30       0.833 TBLADEAF  0         9.08E-02
! *****
!      ATBLDEI1
!===== END AERODYNAMIC COMPONENT =====
!===== BEGIN AERODYNAMIC COMPONENT =====
!      ATBLDEI2
S AEROCO
! Copy ID Source component Destination component
a 1 ATBLDEI1 ATBLDEI2
!      ATBLDEI2
!===== END AERODYNAMIC COMPONENT =====
!      ATROTORI
!===== END AERODYNAMIC SUPERCOMPONENT =====
!===== BEGIN AERODYNAMIC SUPERCOMPONENT =====
!      ATROTORO
s AEROSUPCOMPID
!      IDENTIFY THE SUPERCOMPONENT TO BE EDITED OR CREATED
a ATROTORO
! *****
s SUPCMPTYP
!      DESIGNATE THE SUPERCOMPONENT TYPE
!      Supercomponent Type
!
!      1. Rotor
!      2. Wing
!      3. Body
!      4. Aux. Rotor
!      5. Bailey Rotor
!      6. Ducted Fan
!
a      1
! *****
s COMPID
!      LIST THE AERO COMPONENTS WHICH COMPRISE THE CURRENT SUPERCOMPONENT
!      Aerodynamics Primitive   Auxrotor/   Wing Left   End Wing
!      Component   Structure   Body/Wing   or Blade TIP   Right End
!      Name(s)     Name(s)     Root EL_ID   Node_ID       Node_ID
a      ATBLDEO1    TBLADEO1     0           70           0
a      ATBLDEO2    TBLADEO2     0           70           0
! *****
s CPORIGIN
!      COMPONENT LOCATION WITH RESPECT TO THE SUPERCOMPONENT
!      Component           Component Origin Offset

```

```

!      Name          x          y          z
a      ATBLDE01      0.          0.          0.
a      ATBLDE02      0.          0.          0.
! *****
s CPORIENT
!      COMPONENT ORIENTATION WITH RESPECT TO THE SUPERCOMPONENT
!      Component      rotation 1      rotation 2      rotation 3
!      Name          axis angle(deg)  axis angle(deg)  axis angle(deg)
a      ATBLDE01      3          0.0      2          0.0      0          0.0
a      ATBLDE02      3          -180.     2          0.0      0          0.0
! *****
s SUPCMPTOSS
!      STRUCTURAL SUBSYSTEM ASSOCIATED WITH THE CURRENT SUPERCOMPONENT
!      Subsystem Name
a      TROTORO
! *****
s INFLOW
!      SELECT INFLOW MODEL
!      Inflow Model
!      0. No inflow
!      1. Uniform momentum inflow (half wings and rotors)
!      2. Uniform momentum inflow (full wings)
!      3 Peters and He inflow model (rotors only)
!      4. Wing free wake (Not supported yet)
!      5. Prescribed vortex wake (rotors only)
!      6. Free vortex wake (Scully)
!      7. Wind turbine induction flow (rotors only)
a      1
! *****
s AEROPTION
!      SELECT HIGHER ORDER AERODYNAMIC MODELING OPTIONS
!      Yawed Tip      Linear      Nonlinear      Linear      Compress
!      Flow Loss Unsteady      Unsteady/Dyn Stall      Airfoil      -ibility
!      Effects Option Effects      Leishman-beddos/Onera Coeffs      Effects
!      (0:1)  (0:1)  (0:1)          (0:6)          (0:1)          (0:1)
a      1      1      1          0          0          0
! *****
s TIPLOSS
!      INPUT DATA FOR SIMPLE TIP LOSS
!      Radial Location
!      for Zero Lift
!      (nondim)
a      0.95
! *****
s THRUSTAVE
!      INPUT DATA FOR THRUST AND TIP PATH PLANE ANGLE AVERAGING
!      Thrust Average      # Time Steps      Prescribed      # of Revolutions
!      Option              in Thrust Ave.      Thrust          to Average TPP
a      2                  36                  .000001         1
!===== BEGIN AERODYNAMIC COMPONENT =====
!      ATBLDE01
s AEROCO
!      Copy ID      Source component      Destination component
a      2            ATBLDE11            ATBLDE01
!      ATBLDE01
!===== END AERODYNAMIC COMPONENT =====
!===== BEGIN AERODYNAMIC COMPONENT =====
!      ATBLDE02
s AEROCO
!      Copy ID      Source component      Destination component
a      3            ATBLDE11            ATBLDE02

```

```

!
!==== ATBLDEO2 =====
!==== END AERODYNAMIC COMPONENT =====
!
!==== ATROTORO =====
!==== END AERODYNAMIC SUPERCOMPONENT =====
!====
! Copy aerodynamic components
EXIT
COMMAND
COPYAEROCOMP
COMMAND
!====
!==== ANALYSIS DATA =====
!====
s SELANALYSIS
!
!      SELECT ANALYSIS AND INITIAL CONDITIONS FOR EACH CASE
!      Case ID Trim Mane Stab Init ----- Analysis File Name -----
!      (0:3) (0:1) (0:1) Cond
a      1      1      0      0      D      NO
n
!
!      SPECIFY TITLE FOR EACH CASE
!      Case ID Case Title (Maximum 30 Characters)
a      1      TRIAL2
! *****
s SYSTEMFLAGS
!
!      SELECT SYSTEM LEVEL FLAGS
!      Gravity Aero
!      Effects Effects
a      1      1
! *****
s AEROSTATCONST
!
!      DEFINE AEROSTATIC CONDITIONS
!      Spec_type Vehicle Air Air Speed of
!      (0:4) Altitude Temperature Density Sound
a      4
! *****
!==== TRIM DATA =====
!====
s TRIMVAR
!
!      DEFINE TRIM VARIABLES AND TARGET PARAMETERS
!      Trim TrimVar TrimVar Target TargetValue TargetTol
!      VarID PertValue DampFact ID
a      4      1.      0.5      6      -82.      0.5
! *****
s INTEGPARAM
!
!      INPUT INTEGRATION PARAMETERS
!      No. of Newmark Constants HHT Displace. Velocity Relax.
!      Iter. Alpha Delta Param Tol Tol Factor
a      30 0.1667 0.5 0. 1.E-05 1.E-04 1.
! *****
s CONVERGETOL
!
!      DEFINE PERIODICITY CONVERGENCE PARAMETERS
!      # of # of # of -Displacement Tolerance- --Velocity Tolerance- Min.
!      Trim PSol Time translation rotation translation rotation # of
!      Iter Iter Step (ft) (rad) (ft/sec) (rad/sec) PS Rev
a      100 10 36 0.1 5.E-02 0.5 0.5 5
! *****
s COMPERIOD
!
!      DEFINE THE COMMON PERIOD FOR TRIM
!      Rotor Ratio of Speed
!      Subsystem Common Period to Ratio

```

```

!      Name                      Rotor Period          Tolerance
a      TROTORI                    1                    0.1
! *****
s REASSEMBLE
!      DEFINE FREQUENCY OF ASSEMBLY FOR TRIM
!      Row      Periodic      Solution      Period      Number      Number of Time
!      ID       From         TO          From       TO          Steps Per Assemble
a      1        1            1            1         1            6
! *****

!=====
!===== OUTPUT DATA =====
!=====
s PERIODICOUTPUT
!      SELECT OUTPUT CATEGORY
!      Row      Subsystem      Prim. Struc.      output
!      ID       Name          Name             category
a      1        ALL          ALL              Internal.Loads
! *****
s SAVESC
!      CONTROL SAVING OF SC (SAVED CALCULATIONS)
a RDB                      TRIAL2.SAV

EXIT
M RUNANALYSIS

```

## **Vita**

Lieutenant Commander Mark C. Newkirk graduated from Mayfield High School in Mayfield, Ohio. He entered undergraduate studies at Miami University in Oxford, Ohio where he graduated with a Bachelor of Applied Science in Engineering Management with a technical specialty in Manufacturing Engineering in May 1996. He was commissioned into the United States Navy through the NROTC program at Miami University.

After being designated a Naval Aviator in September 1997, he was assigned to Helicopter Anti-Submarine Squadron TEN (HS-10) for Fleet Replacement Training in the SH-60F Sea Hawk Helicopter, training in Anti-Submarine Warfare, Special Operations, and Combat Search and Rescue Missions. Upon completion, he was ordered to his first fleet squadron, Helicopter Anti-Submarine Squadron FIVE (HS-5) “The Nightdippers.” He deployed with the Eisenhower Battle Group in 2000 and the John F. Kennedy Battle Group in 2002 where he participated in Operation Iron Shield and Operation Enduring Freedom. In March of 2003, he was transferred to Helicopter Combat Support Squadron THREE (HC-3) where he was an Instructor Pilot in the MH-60S. In 2004 he was awarded the Instructor Pilot of the Year amongst his contemporaries. In July of 2005 he entered the Graduate School of Engineering and Management, Air Force Institute of Technology. Upon Graduation, he will be returning to the Fleet as a Department Head in San Diego, CA at Helicopter Anti-Submarine Squadron TWO (HS-2), The Golden Falcons.



<b>REPORT DOCUMENTATION PAGE</b>				Form Approved OMB No. 074-0188	
<p>The public reporting burden for this collection of information is estimated to average 1 hour per response, including the time for reviewing instructions, searching existing data sources, gathering and maintaining the data needed, and completing and reviewing the collection of information. Send comments regarding this burden estimate or any other aspect of the collection of information, including suggestions for reducing this burden to Department of Defense, Washington Headquarters Services, Directorate for Information Operations and Reports (0704-0188), 1215 Jefferson Davis Highway, Suite 1204, Arlington, VA 22202-4302. Respondents should be aware that notwithstanding any other provision of law, no person shall be subject to a penalty for failing to comply with a collection of information if it does not display a currently valid OMB control number.</p> <p><b>PLEASE DO NOT RETURN YOUR FORM TO THE ABOVE ADDRESS.</b></p>					
<b>1. REPORT DATE (DD-MM-YYYY)</b> 14 Jun 07		<b>2. REPORT TYPE</b> Master's Thesis		<b>3. DATES COVERED (From – To)</b> SEPT 05 – Jun 07	
<b>4. TITLE AND SUBTITLE</b>  Process Improvements for the AH-64 Tail Rotor Vibration Analysis				<b>5a. CONTRACT NUMBER</b>	
				<b>5b. GRANT NUMBER</b>	
				<b>5c. PROGRAM ELEMENT NUMBER</b>	
<b>6. AUTHOR(S)</b>  Newkirk, Mark, C., Lieutenant Commander, USN				<b>5d. PROJECT NUMBER</b>	
				<b>5e. TASK NUMBER</b>	
				<b>5f. WORK UNIT NUMBER</b>	
<b>7. PERFORMING ORGANIZATION NAMES(S) AND ADDRESS(S)</b> Air Force Institute of Technology Graduate School of Engineering and Management (AFIT/EN) 2950 Hobson Way WPAFB OH 45433-7765				<b>8. PERFORMING ORGANIZATION REPORT NUMBER</b>  AFIT/GAE/ENY/07-J15	
<b>9. SPONSORING/MONITORING AGENCY NAME(S) AND ADDRESS(ES)</b> DIR, USA RDECOM ATTN: AMSRD-AMR-AE-A (Jon Keller) Bldg 4488 Redstone Arsenal, AL 35898-5000				<b>10. SPONSOR/MONITOR'S ACRONYM(S)</b>	
				<b>11. SPONSOR/MONITOR'S REPORT NUMBER(S)</b>	
<b>12. DISTRIBUTION/AVAILABILITY STATEMENT</b> APPROVED FOR PUBLIC RELEASE; DISTRIBUTION UNLIMITED.					
<b>13. SUPPLEMENTARY NOTES</b>					
<b>14. ABSTRACT</b>  The Apache was the first helicopter of its kind to fly with the tail rotor blade offset by 55 degrees as opposed to the traditional 90 degrees. Current balancing methods approximate the rotor system as a traditional 4 bladed, same plane system with different weight sensitivity coefficients for each set of blades. The Apache tail rotor computer model was built using the Rotorcraft Comprehensive Analysis System (RCAS) program. The objective was not to develop solutions for the sensitivity coefficients, but to identify predictive trends that result from the tail rotor blade location. Currently, sensitivity coefficients applied to the adjustment algorithms of the Aviation Vibration Analyzer (AVA) processor are broken down into an outer blade coefficient and an inner blade coefficient. Evidence from the computer simulation results computed in this research showed that the sensitivities depended on the quadrant the phase fell into, not the relationship between the inner and outer blades. That would mean every blade would have two sensitivity coefficients, one for the adjacent 55 degree quadrant and one for the adjacent 125 degree quadrant. Information collected from RCAS provides enough validation that changes should be made in the process and the next steps should be taken to determining more accurate sensitivity coefficients for the Apache tail rotor balancing procedures.					
<b>15. SUBJECT TERMS</b> AH-64, Helicopter, Tail Rotor					
<b>16. SECURITY CLASSIFICATION OF:</b>			<b>17. LIMITATION OF ABSTRACT</b>  UU	<b>18. NUMBER OF PAGES</b>  97	<b>19a. NAME OF RESPONSIBLE PERSON</b> Donald L. Kunz
REPORT U	ABSTRACT U	c. THIS PAGE U			<b>19b. TELEPHONE NUMBER (Include area code)</b> (937) 255-3636, ext 4548 e-mail: donald.kunz@afit.edu

**Standard Form 298 (Rev: 8-98)**  
Prescribed by ANSI Std. Z39-18